University of Huddersfield Repository

Basha, Majed

Design and implementation of a tuned Analog Receiver for extending VLC
transmission range

Design and implementation of a tuned Analog Front-End for extending VLC transmission range

MAJED BASHA

A thesis submitted to the University of Huddersfield in partial fulfilment of
the requirements for
The degree of MSc by Research

The University of Huddersfield

August 2018

Publication Details

Majed Basha, Design and implementation of a tuned Analog Front-end for extending VLC transmission range", in *IEEE International Conference on Computing, Electronics & Communications Engineering 2018 (iCCECE '18)*, 2018, pp. 173-176.

Abstract: Visible Light Communication (VLC) is challenged by two main drawbacks: ambient light interference and the transmission range. To overcome these drawbacks, we propose an On Off Keying (OOK) based tuned VLC Analog Front-End (AFE) using simple and low-cost electronic circuity. The proposed VLC receiver architecture consists of a Transimpedance amplifier and a fourth order Multiple Feed Back (MFB) band pass filter. The filter is designed with high gain and high-quality factor (Q) for a specified center (resonant) frequency. The system performance was measured in terms of Signal to Noise Ratio (SNR) at two different resonant frequencies. Experimental results show that the proposed VLC front-end is able to extend the transmission range from 60cm to 2.2 m without any form of lensing at either transmitter or receiver. The receiver also showed robustness against ambient light interference. A data rate of 20kbps over a distance of 1.8 m with a bit error rate (BER) $<10^{-9}$ was successfully achieved.

Abstract

Visible Light Communications (VLC) is currently considered one of the most promising Optical Wireless Communications (OWC) for commercial applications, due to the widespread deployment of Light Emitting Diodes (LEDs) for energy efficiency, durability and low cost. With the ability to provide several THz of bandwidth, VLC is expected to co-exist with legacy and future Radio Frequency (RF) media as a reliable solution to the rapid demand of high-speed wireless communication. Most current research on VLC is focused on achieving high data rates over short distances through various types of modulation schemes. Limited research work investigates long range VLC employing high power LEDs, while none of them employed analog filter design in the receiver side while using low power LED for transmission. This thesis work explores the design and easy implementation of a low cost visible light communication system for long-range applications. The main idea of the research is increasing the receiver sensitivity by employing an analog filtering stage within the receiver front-end while the transmission is carried out using a low-power commercial white light LED, enabling the system to provide both illumination and digital communication. The proposed VLC front-end employs a high gain, high Quality (Q) factor band pass filter with the Multiple Feed Back (MFB) topology, which operates at a defined centre frequency range. The proposed MFB active filter uses the gain of the operational amplifier at the defined transmission frequency maximizing the gain and therefore extending the transmission range. The band pass filter behaves as a resonant circuit which detects the desired signal at the transmitting centre frequency and rejects unwanted frequencies including ambient light noise frequencies. Two modulations schemes were used through this work On Off Keying (OOK) with Manchester encoding, and Pulse Width Modulation (PWM). To evaluate the viability of the proposed system several prototypes were designed, implemented and tested. Experimental results demonstrated that by employing the proposed front-end the transmission range could be extended up to 2 m distance by Manchester coding and up to 5 m by using PWM. Moreover, the proposed system showed robustness against ambient light interference under the indoor scenario. Another Arduino prototype was designed and implemented to test the ability of the system to transmit serial data between two PCs. Experimental results demonstrated that the filtering stage is able to improve the receiver sensitivity and extend the transmission distance however, only data rates below 1 kbps were read by the receiver Arduino due to low procession speed of the Arduino boards.

List of Figures

List of Tables

Table of Contents

1. Introduction

In the past decade, world has witnessed a rapid growth in wireless data traffic. The increase in demand for high-speed internet urged the need of further innovation and research to cope with this exponential rise. Currently, Radio Frequency (RF) wireless spectrum suffers from bandwidth deficiency for high data-rate communication therefore, leading to spectrum congestion, which means insufficient bandwidth to be shared among high number of users. Furthermore, RF wireless communication suffer from several drawbacks such as expensive licensing, security issues, and high installation cost in addition to multipath propagation effects in urban environments which reduces its efficiency [1]. Based on these drawbacks an alternative technology is needed to enable continuous indoor wireless communication with the required data rates and increasing demand of users. With an un-licensed bandwidth of ~ 300 THz, Visible Light Communications (VLC) offers a reliable solution, which can overcome the RF limitations. VLC offers superior features over RF, including low-cost with no licensing fee, high bandwidth, high security due to non-interference with electromagnetic waves and energy efficiency. Furthermore, VLC takes full advantage of the existing lighting system which relies on Light Emitting Diodes (LEDs) infrastructure offering the dual use of illumination and data communication. The particular characteristics of VLC systems, enables it to provide solutions for a broad spectrum of applications, including Wireless Local Area Networks (WLAN), indoor localization and positioning systems where current Global Positioning System (GPS) is not available, Intelligent Transportation Systems (ITS), and under water communication offering a range of data rates from a few Kbps up to 10 Gbps. Figure 1.1 shows some VLC practical applications.
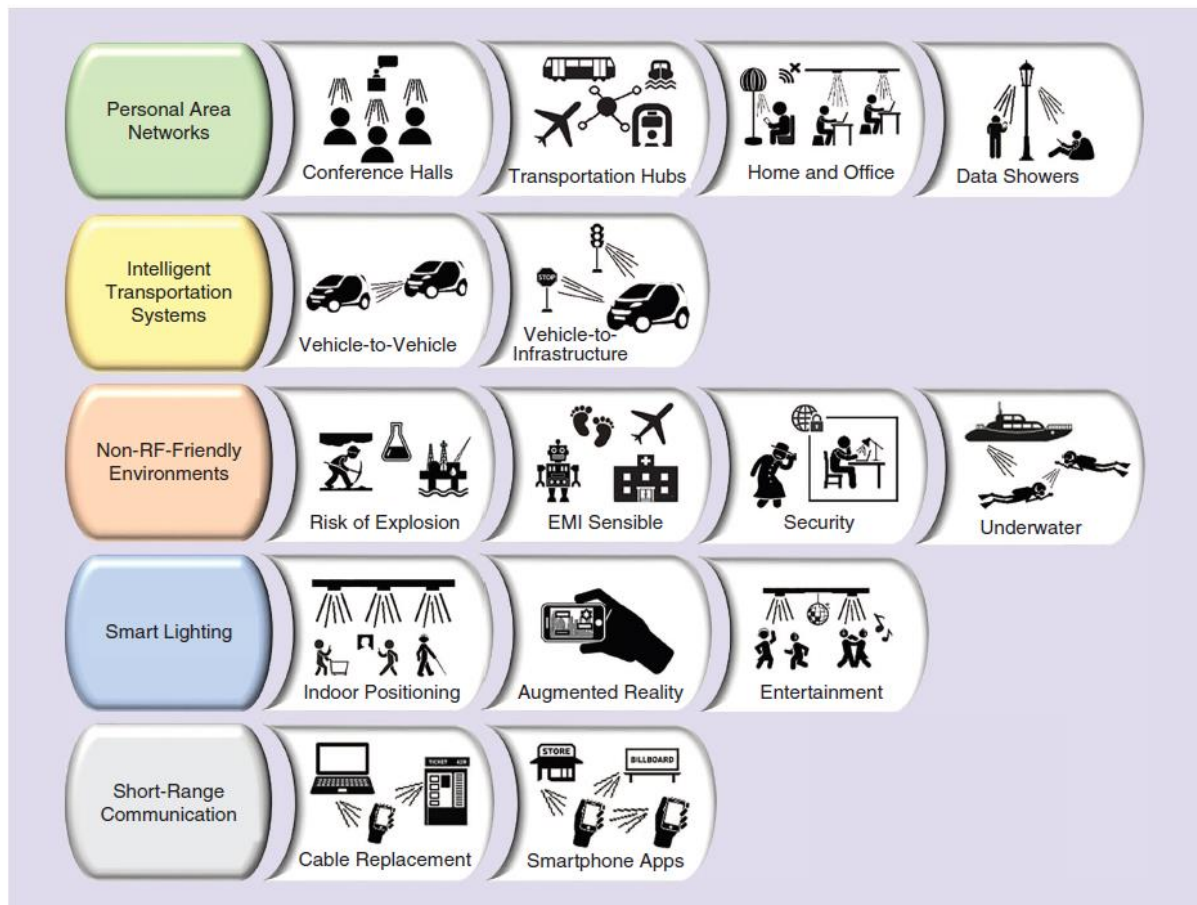
Figure 1.1 Main applications of visible light Communications [2]

1.1. Visible light communication through history

Visible Light Communication (VLC) is the oldest means of communication humankind known. For thousands of years the optical emissions have been used to transmit information, for instance, ancient Greeks used the reflected sunlight to communicate between ships. VLC was first demonstrated by Alexander Graham Bell in 1880 with his invention of the photophone, which was able to transmit a voice signal over a beam of light; its principle of operation was based on modulation of the sunlight focused on a mirror with vibration caused by speech. The photophone vibrating beam was received by a detector where the voice signal was obtained after decoding. Figure 1.2 shows the Graham Bell Photophone 1880. VLC gained more attention after the invention of LEDs because of their ability to be switched on and off in very high speeds. This feature enabled LEDs to achieve high-speed digital communication along with illumination. At frequencies above 100 Hz, the human eye does not recognise the LED

flickering therefore, the light appears to be in a continuous stream. In addition, future lighting is expected to depend on LEDs replacing conventional light sources due to several features: high efficiency, long-life span, and low power consumption [3].
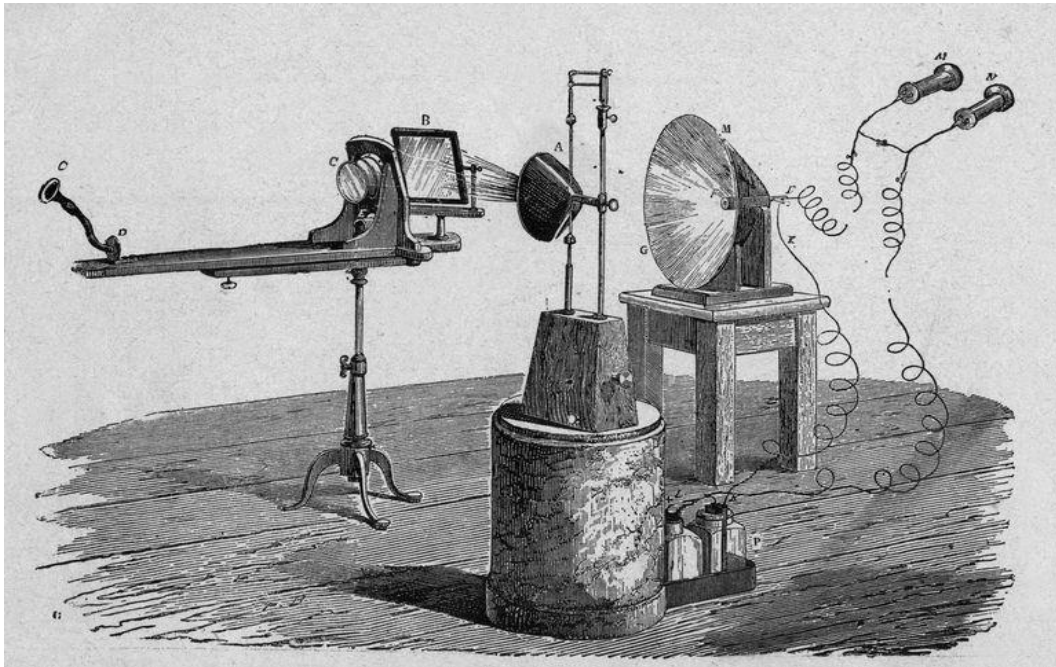
Figure 1.2 Graham Bell Photophone 1880 [4]

1.2. Visible light communication systems

Since 2011 VLC has emerged as an appealing optical wireless communication technology. Visible Light Communication (VLC) gained momentum support after the release of the IEEE 802.15.7 standard which classified different physical layers for indoor and outdoor VLC ranging from 11.67 kb/s to 96 Mb/s [5]. Since then, several researches proved that VLC is capable of achieving Gbps data rates with commercial white LEDs [6]. Through the past couple of years, this technology even attracted more attention from both research community and global society. Figure 1.3 demonstrates this rise by the number of results for the search term "*visible light communication*" conducted using the IEEE *Explore* online library and Google search engine through the last five years. VLC systems are divided in two main categories: Indoor and Outdoor systems.
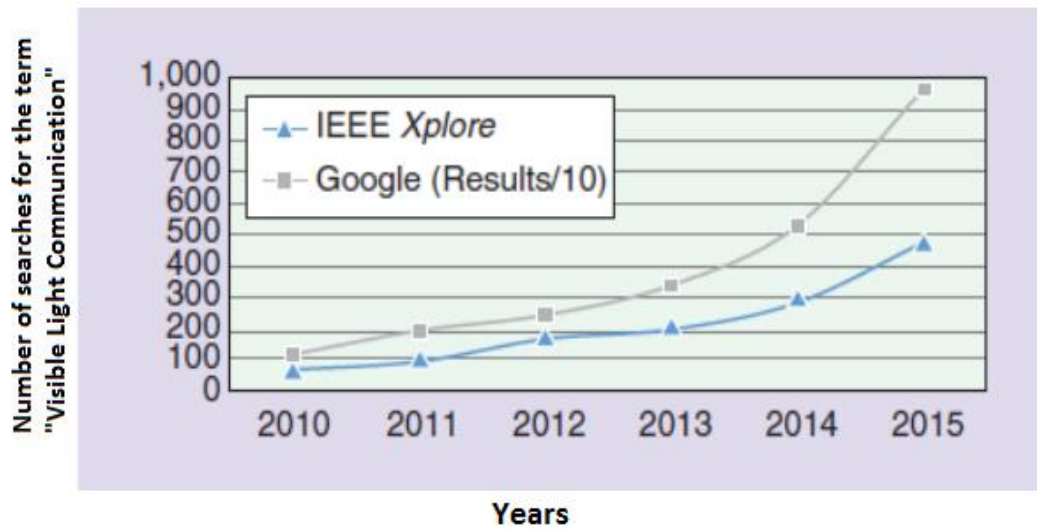
Figure 1.3 Search results for the term 'Visible light communication' using the IEEE Explorer online library and the Google search engine [5]

1.2.1. Indoor systems

Visible Light Communication (VLC) could play a major role in indoor wireless networks including wireless local area networks, wireless personal area networks, and wireless body area networks (WLAN, WPAN, and WBANs). Moreover, indoor VLC systems provide a reliable solution for localization systems and navigation where GPS is unavailable. The dual use of illumination and communication due to the use of the existing LED lighting infrastructure reduces cost and saves energy. Indoor VLC through LED can provide safe and secure solution for communication and localization in several environments where RF based technologies is not suitable or restricted. Some examples are areas where isolation from electromagnetic interference (EMI) is required such as aeroplanes and hospitals. Other environments RF is not desired as it could raise some health concerns such as schools and nurseries [7].

1.2.2. Outdoor systems

In parallel with indoor optical communications, outdoor optical communication was developed which is also known as Free Space Optical (FSO) communication [8]. Optical Wireless Communication (OWC) for outdoor applications supports long communication links

13

1-5 km and short links ranging < 500m links [9, 10]. OWC over Line Of Sight (LOS) channels is able to achieve high data rates up to 10 Gbps [11] however, this feature is traded off by unpredictable weather conditions such as rain, snow, fog and blowing winds. Outdoor VLC was adopted in under water scenarios were RF communication is not suitable with limited data rates . More outdoor applications include intelligent transport systems (ITS) and vehicle-to-vehicle communication which can avoid traffic accidents and improve road safety and management.

1.3. Motivation

Visible Light Communication (VLC) gained popularity through the last decade as a reliable replacement to conventional RF communication due to several factors:

- *Existing LED infrastructure:* With the wide spread of LEDs as the future lighting source, VLC systems could be easily implemented with low cost Front-end components added to the existing infrastructure [12].
- *Low Cost:* Compared to RF communication VLC is lower in implementation cost as it only requires a few upgrades of the current LED lighting system [13]. Besides the free licence visible light bandwidth range which contributes in bringing lower price communication.
- *Moving towards 'Green Technology':* VLC depends mainly on LEDs which are energy efficient light sources which makes VLC emerges as an environmentally friendly communication technology [14]. According to [15] the global electricity consumption will be reduced by 50% if all existing light sources are replaced by LEDs.
- *Interference with RF:* VLC uses visible light spectrum ranging from 390 to 700 nm, between ultraviolet (UV) and infrared (IR) therefore, does not interfere with RF signals [16], which makes it suitable for hospitals and aerospace applications. Since light waves cannot penetrate walls, light communications can offer secure communication zones [17].
- *Wide unlicensed bandwidth:* The visible light frequency spectrum lies between (~400 THz to ~780 THz), while the radio spectrum includes frequency band from (~3 kHz to ~300 GHz) [18] which means that it is 10,000 times greater than RF and currently unused.

14

Finally, with the global wide spread of LED deployment which exceeds 12 billion, and with the ability of converting to potential VLC transmitters, could make the idea of internet of things (IOT) and smart cities achievable.

1.4. Challenges in recent studies

For VLC practical implementation, there is a number of technical challenges which need to be taken in consideration.

1.4.1. Deficiency of modulation bandwidth

Modulation bandwidth is considered one of the key factors of practical Visible Light Communication (VLC) as it decides the transmission data rate. In VLC the modulation band width is limited by the LED bandwidth. White light LEDs used for indoor lighting require a phosphorus coating to convert blue light in to white light, which makes them slower compared to laser diodes and IR LEDs. This physical characteristic limits the LEDs modulation bandwidth to several MHz. To mitigate the LED bandwidth limitation post equalization solution have been proposed [19]. Other solutions including employing various modulation schemes and Multi input Multi output (MIMO) models managed to expand the VLC data rate using white light LEDs up to 10 Gbps [20], [21].

1.4.2. Ambient light interference

One of the main drawbacks in VLC systems is background noise and interference caused by other background light sources such as sunlight, fluorescent lightings and incandescent bulbs which share the same wavelength band. These ambient light sources can significantly interfere with the transmitted signal causing corruption through the optical channel, which affects the received data. To overcome the drawback some hardware solutions were proposed in [22] by employing a high pass filter and a band stop filters at the receiver Front-End.

1.4.3. Transmission range

Transmission range has always been one of the major VLC drawbacks especially in outdoor applications where the communication range is not limited by the room size as in indoor

scenarios. Light intensity decreases rapidly with radiation distance, in addition to scattering and absorption by air particles, therefore, to achieve longer transmission distance, either higher transmission power or higher receiver sensitivity is required which is challenging in practical VLC applications [23].

1.5.   Aim and Objectives

The main target of this research work is to design analog filter circuit to improve the Visible Light Communication (VLC) transmission range and mitigate the effect of ambient light interference in indoor conditions using low power commercial white light LED for transmission taking in consideration the following points:

1. Using low cost available components and simple design architecture.
2. Identify the suitable filtering strategies and modulation schemes to mitigate the effect of ambient light noise under indoor condition.
3. Understanding the manufacturer's characteristics for developing and prototyping a VLC platform determining the user's practical requirements.

1.6.   Contribution of this work

To achieve the above-mentioned objectives, the following steps were taken:

1. Analysing the VLC channel characteristics for LOS condition and understanding the factors that limits the transmission range.
2. Design and simulation of the proposed Analog Front End (AFE) using NI Multisim simulation tool. The proposed VLC front-end employs a high gain and high Quality factor (Q) band pass filter with the Multiple Feed Back (MFB) topology, which operates at a defined centre frequency. The proposed MFB active filter uses the full gain of the operational amplifier at the defined transmission frequency [24] maximizing the gain and therefore extending the transmission range.
3. Mathematical calculations were performed to determine the desired resonant frequencies which will be used during transmission and compared to simulation results.

4. Implementation of the proposed OOK based VLC system and testing the performance in laboratory to evaluate the efficiency while varying the transmission range under the influence of fluorescent lighting.

5. Measuring the viability of the system by analysing the "eye diagram" of the received signal and evaluating the signal to noise ratio (SNR) and bit error rate (BER) at the maximum transmission range.

1.7. Thesis outline

This thesis is structured as follows: Chapter2 covers an overview of Visible Light Communication (VLC) systems including required components for implementations, channel modelling and characteristics. Some of the most popular VLC applications are also discussed in this chapter; In chapter 3 the proposed tuned VLC system for indoor range extension is explained. The design and simulation of both the transmitter and receiver sides is also demonstrated; Chapter 4 and 5 discuss system implementation and experimental results. The experimental tests include two prototypes. The first prototype to be tested in chapter 4 is using OOK modulation and Manchester coding. The second prototype depends on applying the same proposed filter and using PWM which is explained in chapter5; In chapter 6 an Arduino prototype is implemented to test the ability of the VLC system to transmit text data. The designs of transmitter and receiver including suitable algorithms were developed. Experiments were set to test the ability of the system to transmit and receive text data from PC to PC and the system data loss was estimated. Finally, Chapter 7 provides our conclusion and identifies potential points for the future work.

2. Visible Light Communication Theory and Applications

In this chapter, an overview of Visible Light Communication (VLC) system will be given, including the basic components required for VLC system implementation, and the principles of operation. The channel characteristics for an indoor Line Of Sight (LOS) model will be analysed. Modulation schemes which this research is based will also be discussed.

2.1. Light Emitting Diodes

LEDs are P-N junction diodes that are able to produce photonic emission when subjected to electronic excitation. The LED operates in the forward biasing condition by applying an external voltage across the P-N junction. When the forward voltage is applied to the semiconductor material the electrons within the P-N junctions are energized and turned into the (excited state) which is unstable. Energy is released in the form of photonic emission after the electrons return to the stable state. The process of the electronic excitation which causes the transfer of electrons from the conduction band to the valence band is named radiative recombination. Radiative recombination happens when an electron loses energy while passing from the conduction to valence band. The energy of the emitted photon equals the difference between the conduction and valence levels. Figure 2.1 shows the process of Radiative recombination and photon emission [25].
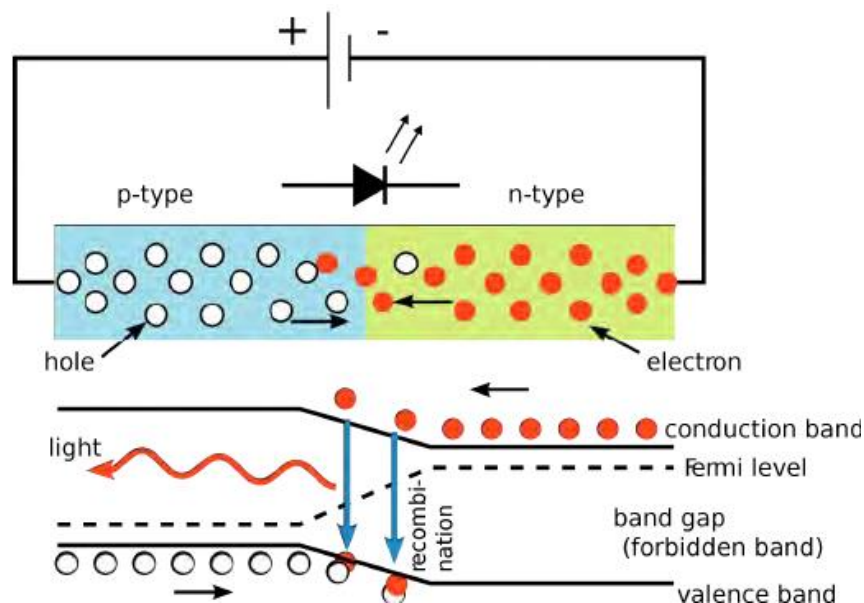
Figure 2.1 The process of Radiative recombination and photon emission [22]

2.2. Photodiodes

The photodiode is a semiconductor device, which generates an electric signal proportional to the amount of light that hits its surface through a process known as photon absorption. The photon absorption is exactly opposite to Radiative recombination by which LEDs generate light. When the semiconductor material in the photodiode is exposed to a light source, the arriving photons provide the electrons in the valence band [26], with the amount of energy required to move to the conduction band. The free photogenerated electrons in the semiconductor can act as charge carriers if an external electric field is applied to the photodiode. The photocurrent I_{ph} generated by the photodiode can be expressed by:

$$I_{ph} = P_o \frac{q\lambda}{hc}(1-r)\left(1-e^{\alpha(\lambda)d}\right) \qquad (2.1)$$

where P_o is the incident optical power, q is the electronic charge, h= 6 626 $\times$ 10^{-34} Js is the Planck's constant, c is the speed of light 3 $\times 10^8$ m/s , λ is the wavelength of the absorbed light, r is the reflection coefficient at the interface air-semiconductor, $\alpha(\lambda)$ is the absorbtion coefficient, and d is the sample length.

2.2.1. Positive-Intrinsic-Negative (PIN) Photodiodes

PIN photodiodes have several advantages over other photodiodes which makes them more suitable for Visible Light Communication (VLC) applications. These features include High sensitivity to visible light spectrum, High response speed and low noise. PIN photodiodes are
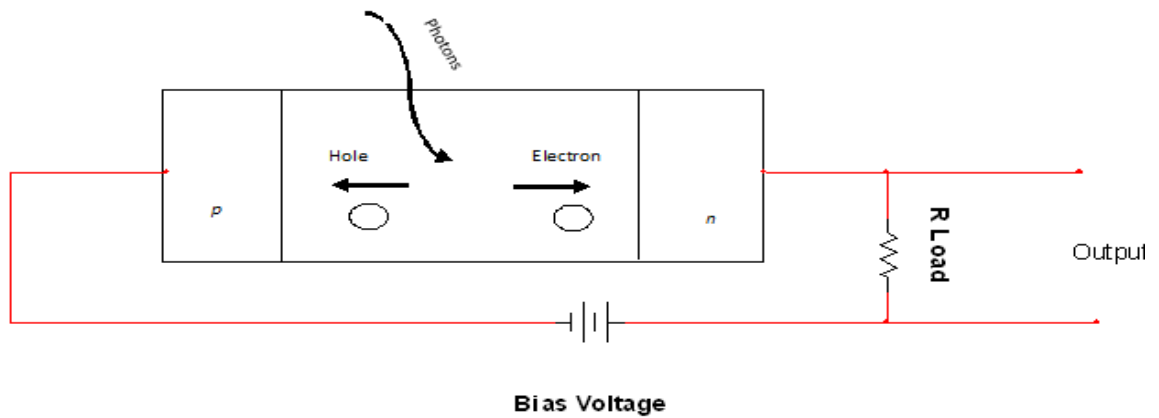
Figure 2.2 PIN photodiode schematic diagram

comprised of P-type and an N-type semiconductor material with an intrinsic layer between them as shown in Figure 2.2. The intrinsic region is a lightly doped semiconductor layer which acts as an optically active region of the device . PIN photodiodes require a reverse bias voltage to ensure that the intrinsic region is depleted from any charge carriers. The photogenerated charge carriers are drifted through the intrinsic layer to the P and N regions generating photocurrent.

2.3. Channel Modelling

To design, implement and operate an efficient optical wireless communication system, it is crucial to understand the channel characteristics. Optical power loss due to channel characteristics depends mainly on path loss and multipath dispersion [27]. The two main configurations considered in VLC are direct LOS and non-LOS configurations. In LOS configuration the reflected light on different surfaces is not taken in consideration, while in non-LOS configuration which is also known as (diffuse channel) the received signal is considered with the reflections of light on different surfaces in the indoor environment. These reflections may cause multipath distortion making it more complex to estimate the path loss model [28]. In this thesis work direct –LOS configuration will be considered.

2.3.1. Channel characteristics for indoor LOS propagation model

In indoor VLC systems, the signal is transmitted using an LED and detected photodiodes. In this case, the Lambertian radiant intensity model. The angular distribution of the intensity model can be expressed as:

$$R_o(\emptyset) = \begin{cases} \frac{(m+1)}{2\pi} cos^m(\emptyset) & for \ \emptyset = [-\pi/2, \ \pi/2] \\ 0, & for \ \emptyset \geq \pi/2 \end{cases} \tag{2.2}$$

Where m is the Lambert's mode number and ϕ is the angle of irradiance. The Lambertian order m is also related to the LED semi-angle at half power $\emptyset_{1/2}$ as seen in equation (2.3).

$$m = \frac{-\ln2}{\ln(cos\emptyset_{1/2})} \tag{2.3}$$

In short range LOS when both the transmitter and receiver are aligned, the light absorption and scattering is too low and can be ignored. In this case the DC channel gain H_{los} can be approximated as:

$$H_{los} = \begin{cases} \frac{A_r(m+1)}{2\pi d^2} cos^m(\emptyset)T_s(\Psi)\cos(\Psi), & 0 \leq \Psi \leq \Psi_c \\ 0, & \end{cases} \tag{2.4}$$

Where A_r is the area of the detector, d is the transmission distance, m is the order of Lambertian emission, $\emptyset$ is the angle of irradiance, Ψ is the receiver angle of incidence, Ψ_c is the receivers' field of view (FOV), and $T_s(\Psi)$ is the transmission response of the optical system. According to (2.4) the channel gain is inversely proportional to the transmission distance.
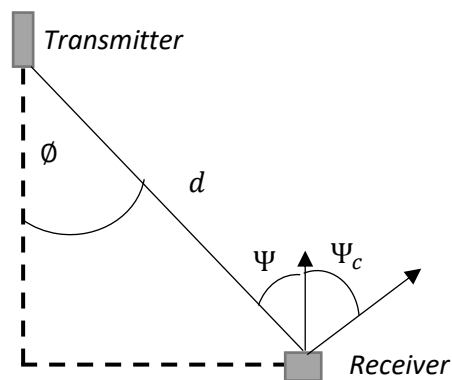
Figure 2.3 Geometry of LOS propagation

In longer distance VLC, the transmitted signal will be affected by atmosphere absorption and light scattering, which deeply reduces the channel gain. The monolithic channel gain due to attenuation of light intensity H_{owc} can be defined as:

$$H_{owc} = H_{los}(\lambda)\exp(-\beta(\lambda).d) \tag{2.5}$$

$$\beta(\lambda) = \alpha_m + \alpha_a + \sigma_m + \sigma_a \tag{2.6}$$

Where $\beta(\lambda)$ is the attenuation coefficient, α_m is the atmospheric absorption coefficient, α_a is the absorption coefficient of aerosol particles, σ_m is the scattering coefficient of atmospheric molecules, and σ_a is the scattering coefficient of aerosol particles. From the above equations, we can conclude that by increasing the transmission distance, the channel gain will decrease, which means that long-range VLC applications will suffer from low SNR. Therefore, to achieve longer transmission distance, higher transmission power and higher receiver sensitivity are needed which is challenging in practical VLC applications.

2.4. Modulation schemes

In VLC the LED transmission is performed by Intensity Modulation (IM), while reception is carried out by photodiode through Direct Detection (DD). Figure 2.4 shows the block diagram of an optical intensity, direct detection VLC communication channel.
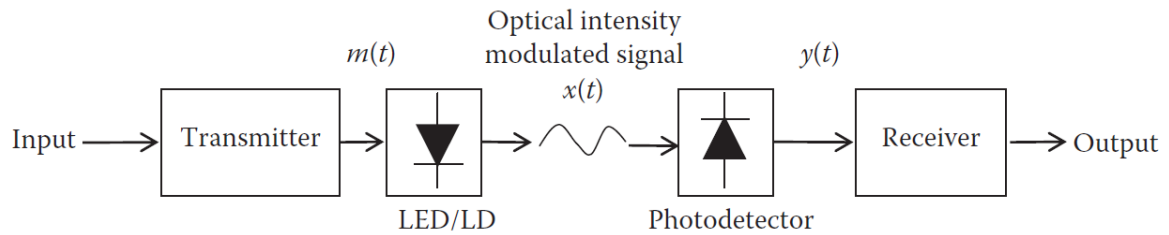
Figure 2.3.1.4 Optical Intensity and direct detection VLC channel

The optical intensity should be a real nonnegative value; this forms some constraints on which modulation schemes are favourable in VLC. Generally, there are two main categories of modulation used in VLC, which are single-carrier and multi-carrier modulation. Some of the single carrier modulation techniques applied to VLC are Pulse modulation amplitude (PAM) which is popularly known as on off keying (OOK), Pulse position modulation (PPM), and Pulse width modulation (PWM). Multicarrier modulation schemes include Orthogonal Frequency Division Multiplexing (OFDM). In terms of high data rates OFDM is considered more efficient than single carrier modulation schemes however, OFDM has high Peak to Average Power Ratio (PAPR), which causes dimming effect on the LED and therefore affects the lighting

system [29]. Moreover, compared to OOK, OFDM hardware implementation is very complex and expensive which makes it wasteful if used for low data rates applications. In this section OOK, Manchester encoding and PWM which are involved in this research will be discussed.

2.4.1. On Off Keying

On Off Keying (OOK) is the most common single-carrier modulation scheme widely used in VLC implementation is due to its advantages of low complexity, low cost, and power efficiency [30]. In OOK LEDs are turned on or off according to the data bits being 1 or 0. A binary '1' is represented by an optical pulse which occupies the duration while a binary '0' is represented by the absence of the optical pulse. OOK modulation have been standardised in IEEE 802.15.7 for both indoor and outdoor applications. OOK can be categorized in two main configurations either Return to Zero (RZ) or Non Return to Zero (NRZ) schemes. In NRZ scheme the binary '1' is represented by a pulse with a duration equal to the transmitted bit duration, while in RZ scheme only a partition of the transmitted bit occupies the pulse. Figure 2.5 shows time waveform of (a) OOK-NRZ and (b) OOK-RZ with a duty cycle of $\gamma = 0.5$ and for an average transmitted power P_t and with a bit duration T_b .
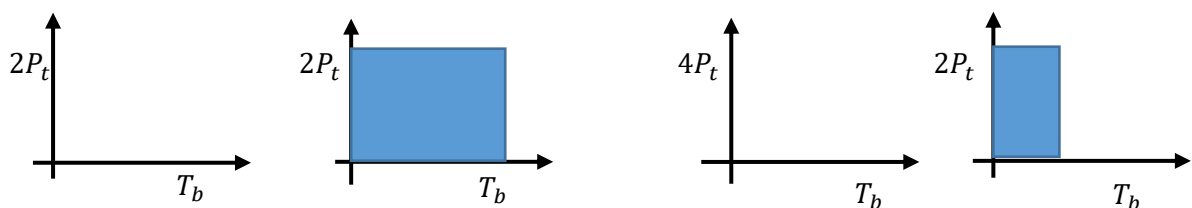
Figure 2.5 Time pulse of (a) OOK-NRZ (b) OOK-RZ

2.4.2. Manchester encoding

Manchester coding is one of the most common data coding methods used in conjunction with OOK in communication systems. The IEEE 802.15.7 standardized Manchester coding for

visible light communication, as one of the Run-length limited (RLL) codes which were defined to avoid long runs of 1's and 0's that could potentially cause flickering and Clock and Data Recovery (CDR) detection problems [31]. LED flickering happens when long sequences of ones or zeros are transmitted by the LED. In Manchester encoding each bit send as a transition from high to low state is represented by '1' and any transition from low to high state is represented by '0'. By this process always, an equal number of ones and zeros are sent which solves the flickering problem. Figure 2.6 shows a Manchester encoded signal formed by embedding a clock in to the data stream. However, in Manchester coding each logical data bit is divided into two physical bits, this causes the data rate to be halved compared to OOK.
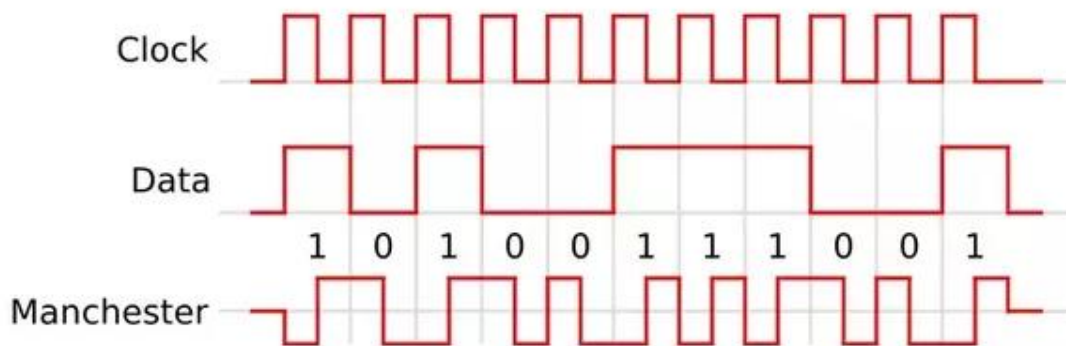
Figure 2.6 Manchester encoding

2.4.3. Pulse width Modulation

Pulse width modulation (PWM) is a type of pulse time modulations where the signal variation occurs in the width of the pulse. The PWM signal consists of a periodic train of rectangular pulses, whose widths are adjustable, consequently resulting in the variation of the DC level of the waveform [32]. PWM is widely used in VLC for LED dimming control. In modern lighting systems, dimming control is essential. As VLC systems are based on LED illumination, PWM is the most effective modulation scheme, which can be used to accurately control LED dimming without incurring colour rendering of the emitted light.

2.5. Visible Light Communication Applications

The ability of VLC systems to provide illumination along with data communication makes it a reliable solution for a wide range of applications. This chapter will provide some of these applications along with the progress made in practical implementation.

2.5.1. Intelligent transport systems

Figure 2.7 Vehicle to Vehicle and Vehicle to Infrastructure Communication

Recently traditional street lightings which are based on incandescent and fluorescent lamps are being replaced by LED lighting due to high efficiency and low power consumption. This gives a high chance of incorporating VLC in Intelligent transport systems (ITS) depending on the existing LED lighting infrastructure. As shown in Figure 2.7 this technology can be adopted for both Vehicle to Vehicle (V2V) communication and Vehicle to Infrastructure (V2I) communication. ITS can improve road safety, avoid car accidents and maintain efficient traffic systems [33]. However, there is a number of difficulties which faces deploying this technology in practical outdoor scenarios, and further research is required to improve coverage link and robustness during different weather conditions. One of the major difficulties in V2V communication is that both the transmitter and receiver have to communicate while in

motion. In V2V communication most research studies propose high-speed cameras for reception. The advantage of high-speed cameras is that they enable tracking because the data is carried on pixels of the LED array on the transmitter. Application of high speed cameras in ITS is not feasible due to the complexity of image processing demodulation and high cost of the cameras. VLC could provide a reliable and low cost solution for ITS by applying further research to overcome its drawbacks in outdoor scenarios [34].

2.5.2. Positioning and Localization

The application of VLC for indoor positioning systems have been attracting researcher's attention during the past decade due to its ability to support accurate locating in the indoor environment using the existing LED lighting infrastructure. The current GPS which is used in various outdoor applications such as car and mobile navigation is not able to provide positioning within indoor environment as GPS depends on the signals received from Satellites which are blocked by buildings [35]. Other indoor positioning techniques have been proposed such as Radio Frequency Identification (RFID), Wireless Local Area Network (WLAN), and Infra-Red (IR) However they suffer from a number of drawbacks such as system instability due to multipath propagation, low accuracy and long-time response [36]. Compared to other systems VLC based positioning systems are favourable due to the following advantages:

- VLC employs LEDs which provide a narrow beam width and therefore gives a precise Angle of Arrival (AOA) at the receiver front-end.
- VLC mainly depends on LOS therefore, is less affected by multipath interference.
- VLC-based positioning can be used safely in non-RF- Friendly environments such as hospitals, aircrafts, and mines.
- Since VLC utilizes existing LED lighting, positioning systems could be easily implemented by applying low cost upgrades to the current lighting system.

VLC- Based positioning gained high interest from shopping centres and malls due to its ability to maximise the revenue and facilitate supply chains. The demand on VLC based indoor positioning for retailers and shopping centres is expected to reach $5 Billion by the end of this decade [37].

2.5.3. Under water communication
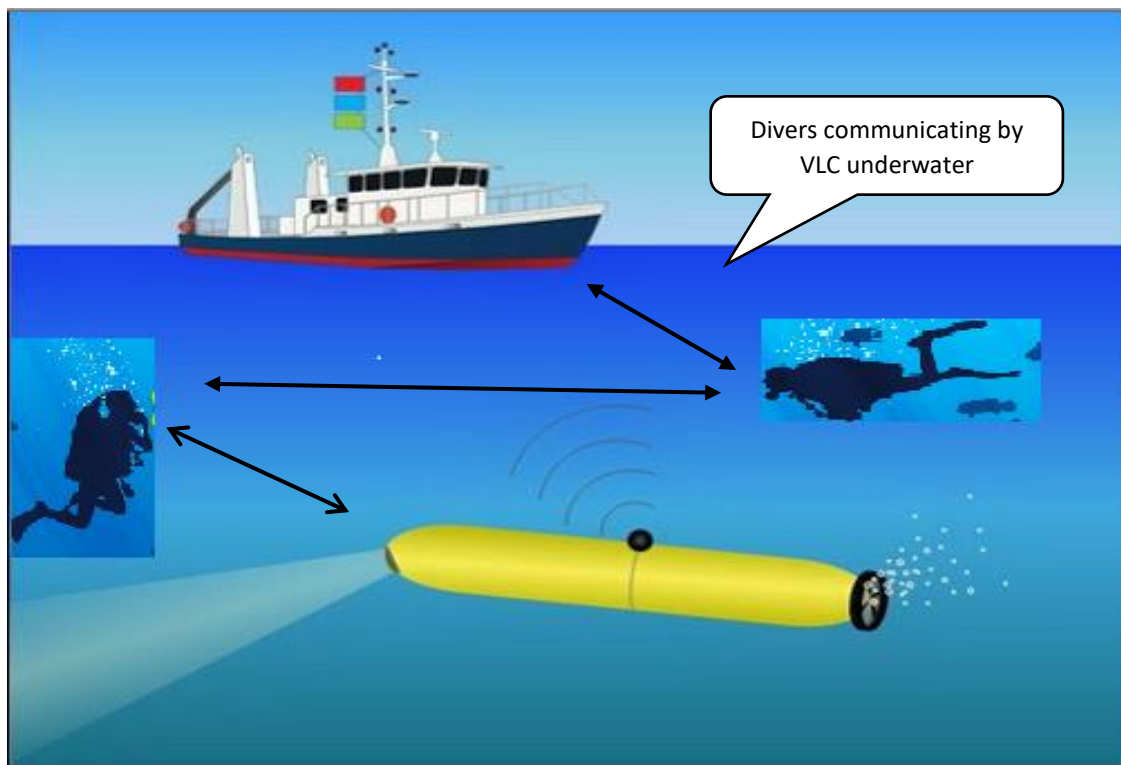
Figure 2.8 Underwater VLC applications

Nowadays, underwater wireless communication gained great interest in military, industry, and the scientific research. Figure 2.8 shows how VLC can be used by divers to communicate to each other and to ships or submarines. VLC have been proposed as an alternative way of underwater communication due to its high speed, low power consumption and wide bandwidth. RF technology has extremely high attenuation and limited coverage distance in seawater and Acoustic (Sonar) communication has limited data rate of 10 Kbps due to the low speed of Acoustic waves. In addition, Acoustic communication is expensive to implement. However, due to water characteristics underwater VLC is also faced by some drawbacks which limits its performance including absorption and scattering [38]. Light absorption tend to be higher in the red part of the spectrum (wave length 450 nm) in clear water condition which could change according to the type of impurities contained in the water [39]. Several studies have been proposed to mitigate Underwater VLC fading. In [40] an Underwater VLC system employing an optical pre-amplifier with spatial diversity and OOK modulation was demonstrated. A mathematical model of vertical Underwater VLC system for both LOS and

NLOS conditions was presented in [41]. Another study proposed a long distance Underwater VLC system with a single photon avalanche diode (SPAD) employed at the receiver to improve the detection sensitivity [42].

3. Design and simulation of a tuned VLC analog front-end

In this chapter, we propose a tuned VLC system for long range indoor applications. To design this system, we first chose the suitable low cost components which will be used to implement the VLC system according to their technical characteristics, then simulation is performed to evaluate the viability of the proposed prototype. The first two sections of this chapter will demonstrate the proposed VLC system block diagram and a brief description of VLC platform parameters and specifications. The following sections will describe in details the design and simulation of both the transmitter and receiver sides.

3.1. VLC System Block Diagram

Figure 3.1 shows the block diagram of the proposed VLC system. The transmitter (Tx) is comprised of a signal generator and the LED driver circuit. The data generated by the signal generator will be encoded and transmitted by the diver circuit using OOK modulation and Manchester encoding. Next, the data is transmitted by visible light, which is emitted by white light LED. At the receiver (Rx) side the signal is detected by the photodiode. Due to the communication channel characteristics, the data received at the Rx side is faded, attenuated, and interfered with ambient light noise. In order to reduce the noise interference and increase the receiver sensitivity we propose a receiver design, which is comprised of a Transimpedance Amplifier (TIA) and, a fourth order band pass filter with MFB topology. Finally, the received signal is observed and analysed through the oscilloscope.
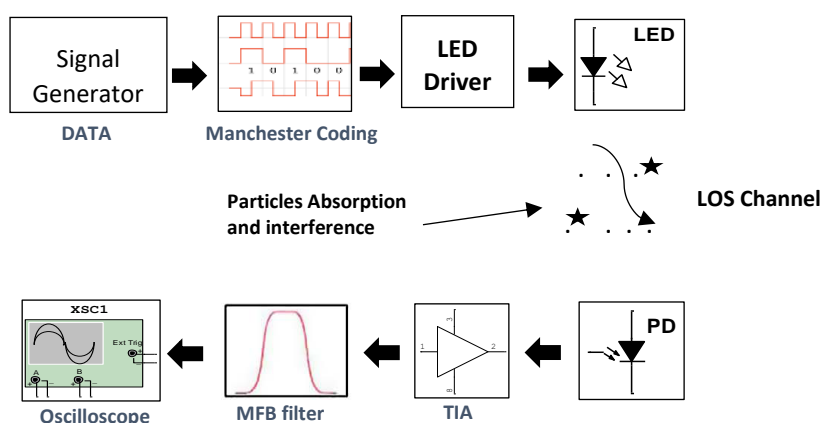
Figure 3.1 The block diagram of the proposed VLC system

3.2. VLC platform parameters and specifications

The main goal of the experiments is to improve the transmission range of a Visible Light Communication (VLC) system using a low power white light LED for transmission within the indoor laboratory environment under the influence of fluorescent lights. The electronic components were carefully chosen to meet the system requirements. A low cost commercial white light Nichia (NSDL570GS-K1) 0.2 Watts power LED with half power angle of 70 degrees, biased at 100mA was chosen. Nichia LEDs have the advantages of durability, homogeneity and brightness, which makes it suitable for dual purpose of illumination in addition to data communication. The radiation pattern and wavelength characteristics of the Nichia (NSDL570GS-K1) LED used in the experiments are shown in Figures 3.2 and 3.3 [43]. The LED relative radiant intensity peaks at the wave length of 590 nm.
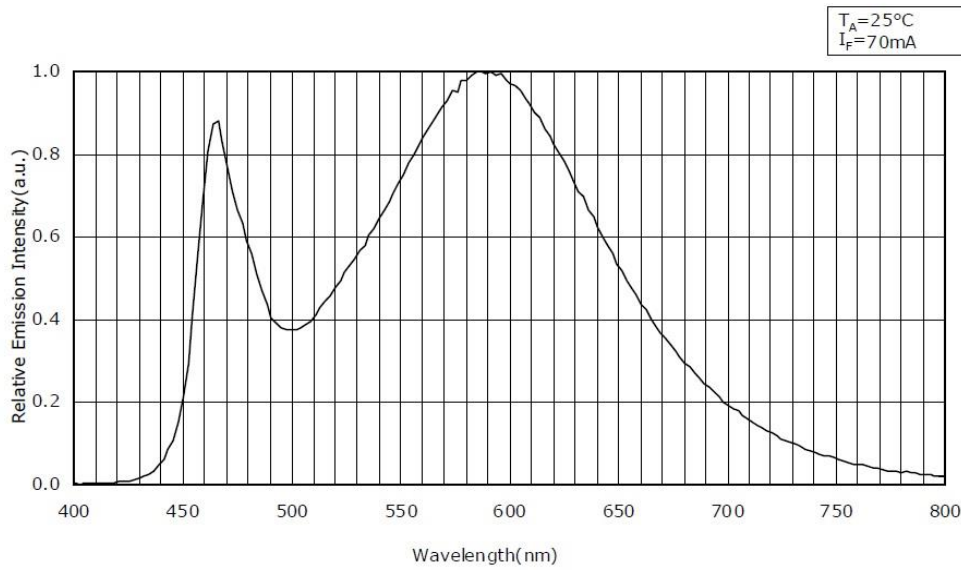
Figure 3.2 LED wavelength characteristics [38]
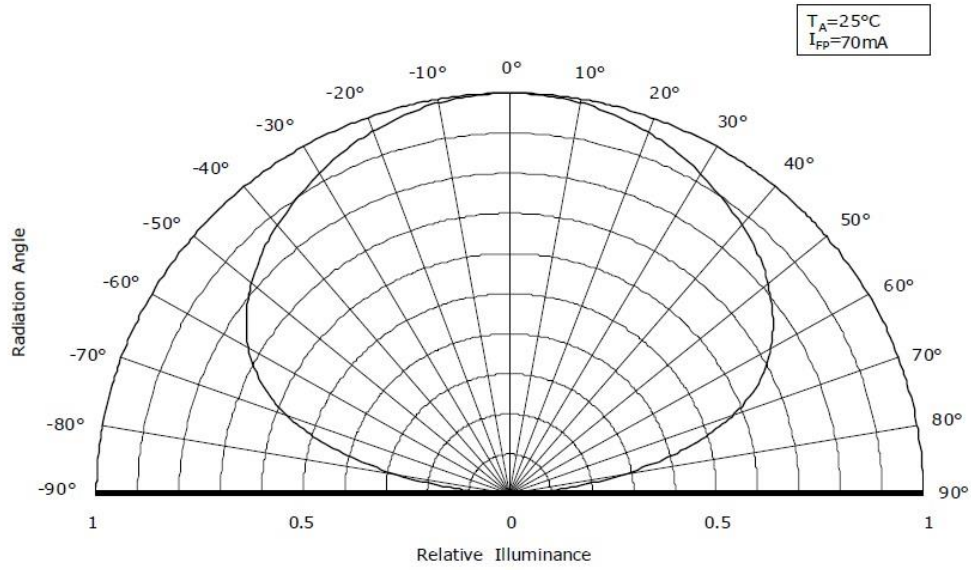
Figure 3.3 LED Radiation pattern [38]

At the receiver, the chosen photodiode was the VTB8440BH Silicon photodiode with infrared rejection filter to mitigate the effect of ambient interference. The photodiode has a spectral response, which is only influenced by visible light, making it suitable for this application. This photodiode also has the advantages of high speed and low noise due to its low junction capacitance and low dark current. The Op-amp used for the Transimpedance amplifier and the active filter was the LT1056 JFET input operational amplifier. This Op-amp was chosen with a gain bandwidth product of 6.5 MHz due to the Multiple Feedback (MFB) minimum gain bandwidth product requirement, so that the filter will not oscillate. The LT1056 Op-amp is also suitable to be used as a photodiode amplifier due to its low input bias current. Table 3.1 shows the components parameters used in experiments.

Table 3.1 VLC platform parameters and specifications

Variable	Description
Application	Indoor
Maximum Coverage range	2.2 m
Configuration	Direct LOS link
Maximum Bitrate	30 Kbps
Modulation	Manchester encoding
Transmitter	LED Specification: • Nichia 510G White LED • Power dissipation: 270m W(max) • View angle: 120° • Luminous Flux: 25.5 lm • Wavelength: 380-760 nm (white)
Receiver	Photodiode specifications: • VTB8440BH Silicon photodiode with infrared rejection filter • Spectral response: 330 – 720 nm • Effective area size: 5.16 mm^2 • Dark Current at reverse voltage V_R = 10v: ID=10 nA • Junction Capacitance at reverse voltage V_R = 0v, 1MHz: Cj=18 pF
OP-AMP	• LT1056 JFET input operational amplifier • dual supply ±2.5 V_{DC} • Gain bandwidth product 6.5 MHz
Interference lamp	Fluorescent tube lights

3.3.   Transmitter Design

The proposed transmitter is comprised of two stages: The Manchester encoding stage and the LED driver circuit. Figure (10) shows the schematic diagram of the proposed transmitter circuit.

3.3.1. Manchester encoding

As explained in the previous chapters Manchester encoding was chosen as it is a simple digital serial data encoding method which generates arbitrary bit patterns without any long strings of continuous zeros or ones and therefore, maintaining DC stability and avoiding Inter Symbol Interference (ISI) at the receiver side. Manchester encoding is simply performed by logically combining the Pseudo Random Binary Sequence (PRBS) generated by the signal generator and a data-rate clock using an X-OR gate. As shown in Figure 3.4 the first waveform is a clock signal and the second wave form is the PRBS signal from the function generator and the third signal is the Manchester coded signal at the output of the X-OR gate.
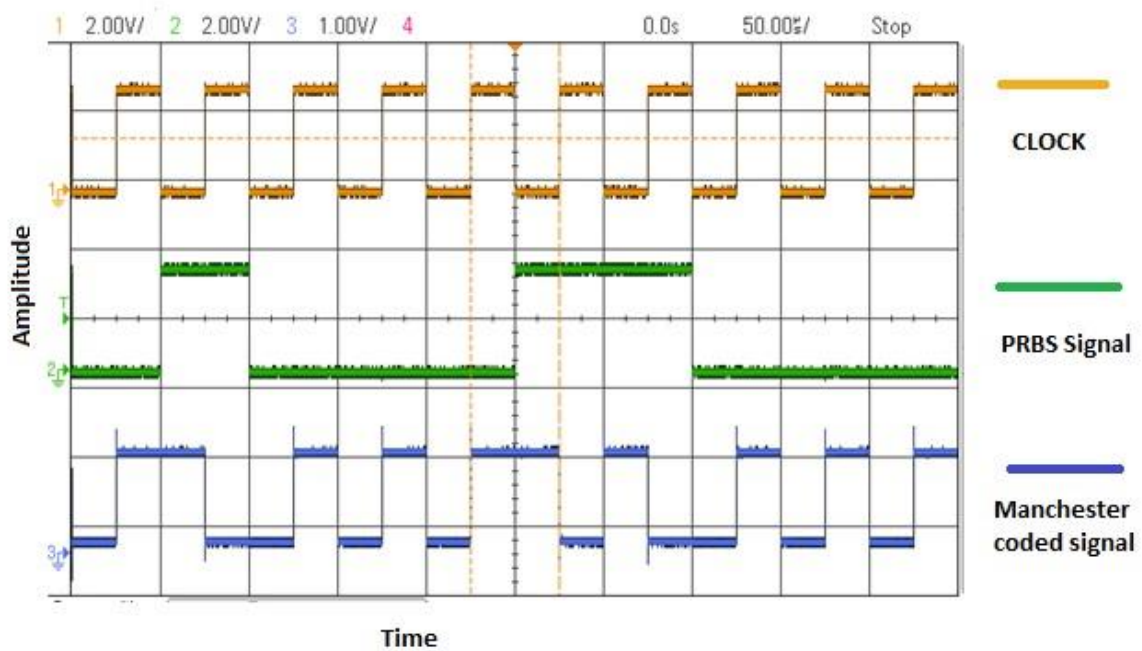
Figure 3.4 Generated Manchester coded signal

3.3.2. LED driver circuit

As shown in Figure 3.5 the LED driver circuit was designed using the Common-Collector (CC) transistor configuration. The high input impedance and low output impedance with an approximate unity gain of the CC configuration makes it a good choice as a buffer in the

Transmitter design [44]. The resistors R_1 and R_2 form a voltage divider that controls the base emitter voltage. The coupling capacitor C_1 blocks any DC signal at the input. The resistor R_3 controls the LED forward current and R_4 degenerates the emitter for early voltage improvement.
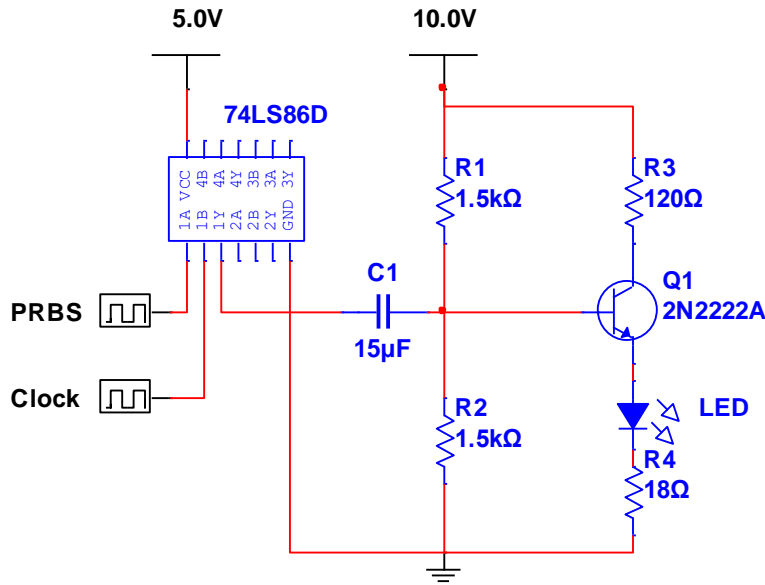
Figure 3.5 Schematic diagram of the OOK VLC transmitter

3.4. Receiver design

The proposed receiver front-end is comprised of a photodiode, Transimpedance Amplifier (TIA) and a MFB band pass filter. In this section, the function of each stage will be explained.

3.4.1. The Transimpedance Amplifier

The simplest way to implement a Transimpedance amplifier (TIA) is by using an Op-Amp with a large value feedback resistor (R_f). The TIA amplifies the small photocurrent generated by the photodiode and converts it in to usable voltage. The TIA gain is controlled by the value of the feedback resistor however; this is traded off by Op-Amp noise. When an incident light is applied to the photodiode a photocurrent proportional to the light intensity is generated and flows through the feedback resistor which converts the current to a voltage given by:

$$V_{out} = -R_f . I_p \qquad (3.1)$$

34

The TIA is an essential building block in optical receiver where the current to voltage conversion occurs in addition, the system speed is decided by the TIA available bandwidth. The LT1056 Precision JFET Input Op-Amp chosen for the proposed TIA due to its low cost, sufficient bandwidth and high performance as a photodiode amplifier. As shown in Figure 3.6 the TIA stage is comprised of the LT1056 Op-Amp, feedback resistor R_f and bias resistors R_{b1} & R_{b2}. The LT1056 Op-Amp has an internal capacitance of ($C_{in \approx 4pF}$). During operation, the resistive feedback with the source resistance and capacitance creates a phase shift and oscillation. By adding, a small capacitor C_f in parallel with R_f eliminates this problem and helps removing the noise at the photodiode output [45].
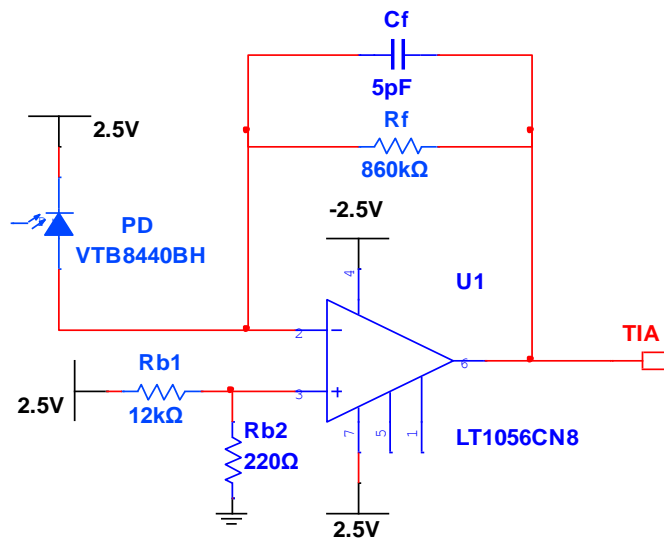
Figure 3.6 TIA Schematic Diagram

3.4.2. The Multiple feedback band pass filter

The proposed filtering stage is a fourth order Butterworth MFB active band pass filter with high gain, which comprises of two second order filters in cascade as shown in Figure 3.7 This topology was chosen due to its simplicity in design and its ability to achieve high gain at the specified center frequency [46]. This type of active band pass design produces a "tuned" circuit based around a negative feedback active filter giving it a steep roll-off on either side of its center frequency. The frequency response of the filter is similar to a resonance circuit with high gain and high Q at its center frequency. The Quality factor of the filter is determined by

35

the overall width of the pass band between the upper and lower -3dB corner points. In other words, the Q factor measures the selectivity of the band pass filter, however this trades off the filter's bandwidth. In order to achieve the highest possible gain at the defined center frequency, the two second order stages of the filter were designed to be in synchronized tuning assuming identical component values. Each second order MFB band pass filter stage has the following transfer function:

$$A(s) = \frac{\frac{R_2 R_3}{(R_1+R_3)}.C.\omega_m.s}{1+\left[\left\{\frac{2R_1 R_3}{(R_1+R_3)}.C.\omega_m\right\}s\right]+\left[\left\{\frac{R_1 R_2 R_3}{R_1+R_2}.C^2.\omega^2\right\}.s^2\right]}$$

(3.2)

Where; (ω_m) is the angular mid-frequency of the filter.
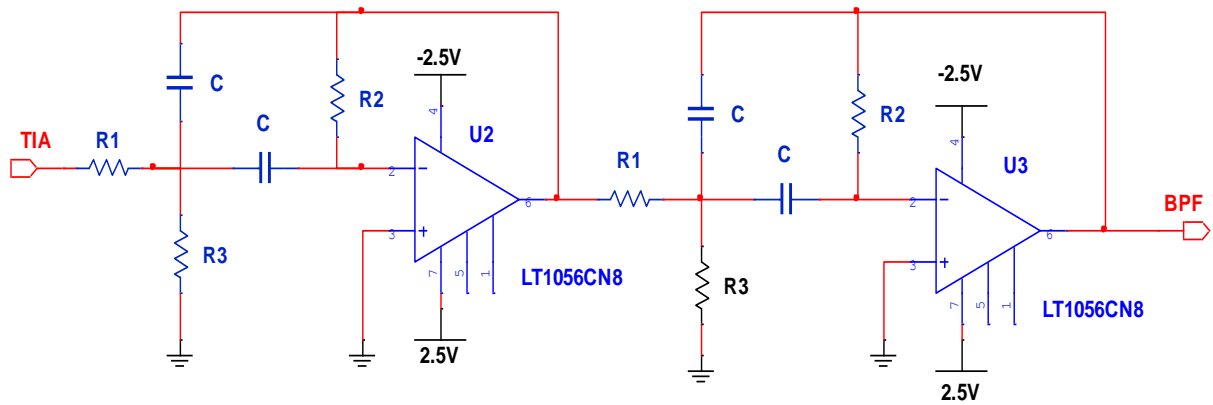
Figure 3.7 Schematic Diagram of 4th Order MFB filtering stage

The MFB filter allows adjusting the mid-frequency (f_m), the gain at mid-frequency (A_m), and the Q Factor independently as defined by (3.3), (3.4), and (3.5).

$$f_m = \frac{1}{2\pi C}\sqrt{\frac{R_1+R_3}{R_1 R_2 R_3}}$$

(3.3)

36

$$A_m = -\frac{R_2}{2R_1} \tag{3.4}$$

$$Q = \pi f_m R_2 C \tag{3.5}$$

3.4.3. Filter design and simulation

To evaluate the viability of the proposed MFB filtering stage two operating mid-frequencies were chosen 5 kHz and 10 kHz. The resistor values for each design were obtained by using equations (3.3), (3.4) and (3.5). Table 3.2 shows the calculated values of the MFB filter components assuming the filter's Q factors $Q \approx 10$ and the required gain at the mid-frequency is $A_m \approx 54\ dB$.

Table 3.2 Values of MFB filter components

f_m	Components/parameter and Values				
	R_1	R_2	R_3	C	Gain
5 KHz	220 Ω	220 KΩ	120 Ω	4.7 n	54 dB
10 KHz	220 Ω	220 KΩ	120 Ω	2.2 n	

The proposed MFB band pass filter achieves its maximum gain at its center frequency which is the same frequency used during transmission. Therefore, strengthening the detected signal by increasing the receiver's sensitivity at the chosen frequency and therefore, extending the transmission range. Another advantage of the MFB band pass filter is its rejection to unwanted frequency bands including ambient light sources. Indoor VLC systems suffer from shot noise caused by the ambient light resulting from both artificial and natural sources. Conventional fluorescent lamps introduce sinusoidal signals with frequency that ranges between 20 kHz-50 kHz and can also produce frequencies of 50 Hz-100 Hz or 1MHz if they are driven by electronic ballasts [47]. In this case, the use of a high pass filter will not be a good choice as the high frequency harmonics will still disturb the received signal. Figure 3.8 shows the simulation results for the frequency response of the 4th order MFB filter designed for 5

kHz and 10 kHz. Simulation was carried using NI Multisim simulation tool. The filter has a pass band bandwidth of 1kHz with a great pass band gain of 54 dB and roll off rates of -40 dB/dec & 40 dB/dec. From the frequency response graph, we can see that the 4th order MFB band pass filter with Butterworth response can satisfy the system requirements.
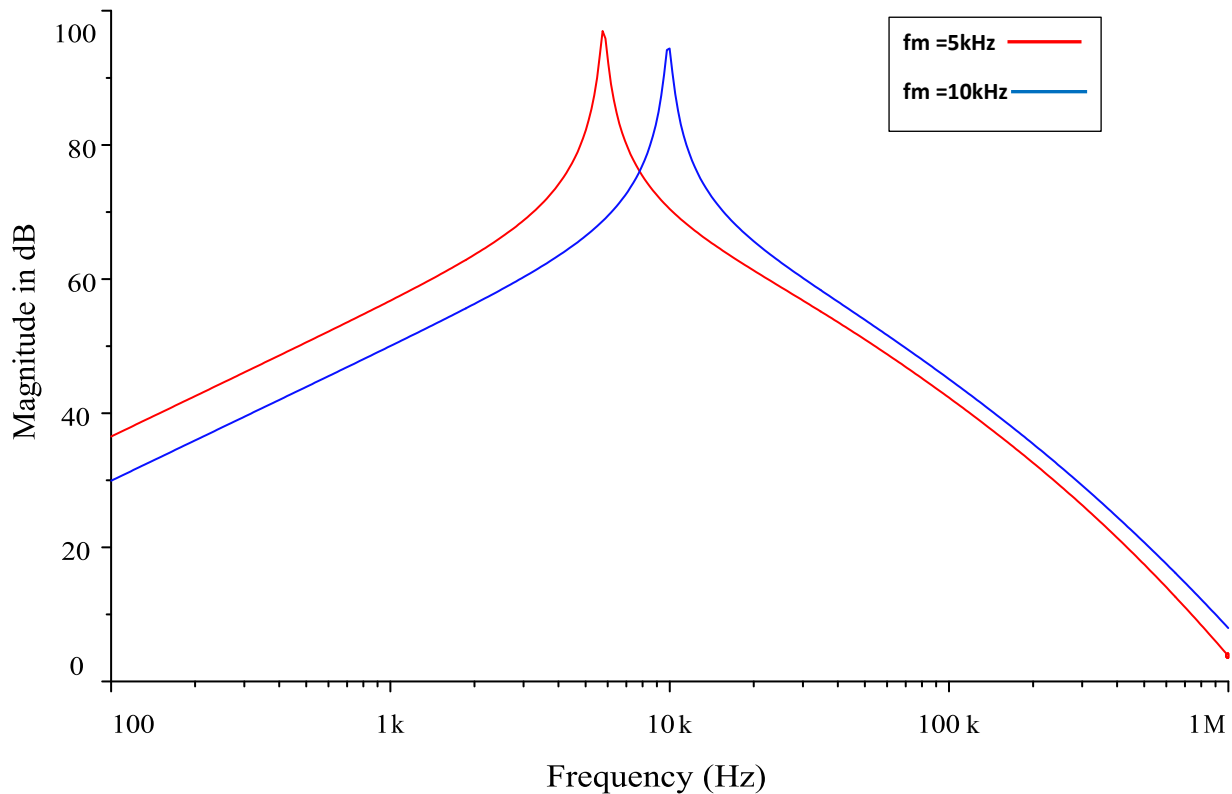
Figure 3.8 Frequency response of the MFB band pass filter
at frequencies fm=5 kHz & fm=10 kHz

3.4.4. Simulation of the proposed VLC receiver

Transient simulation was carried to the whole VLC receiver front-end. As the photodiode could not be simulated using NI Multisim it has been replaced by a pulse current source. The photocurrent detected by the photodiode was assumed to be 200nA pk-pk and two designs for the two resonant frequencies of 5kHz and 10kHz as shown in figures 3.9 & 3.10 were simulated.
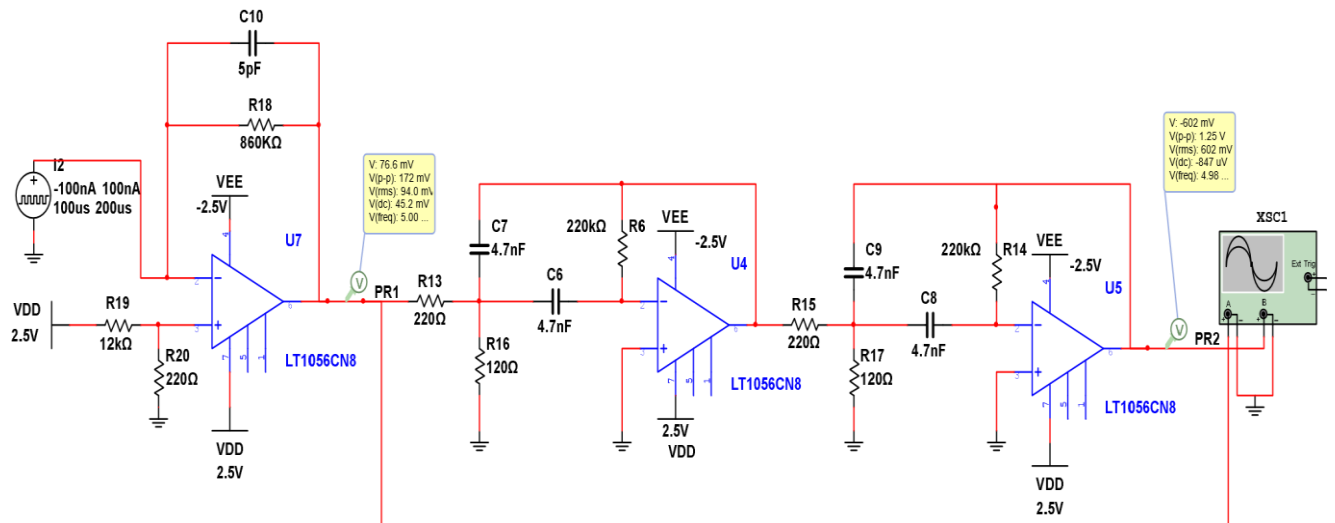
Figure 3.9 VLC receiver for resonant frequency of 5 kHz
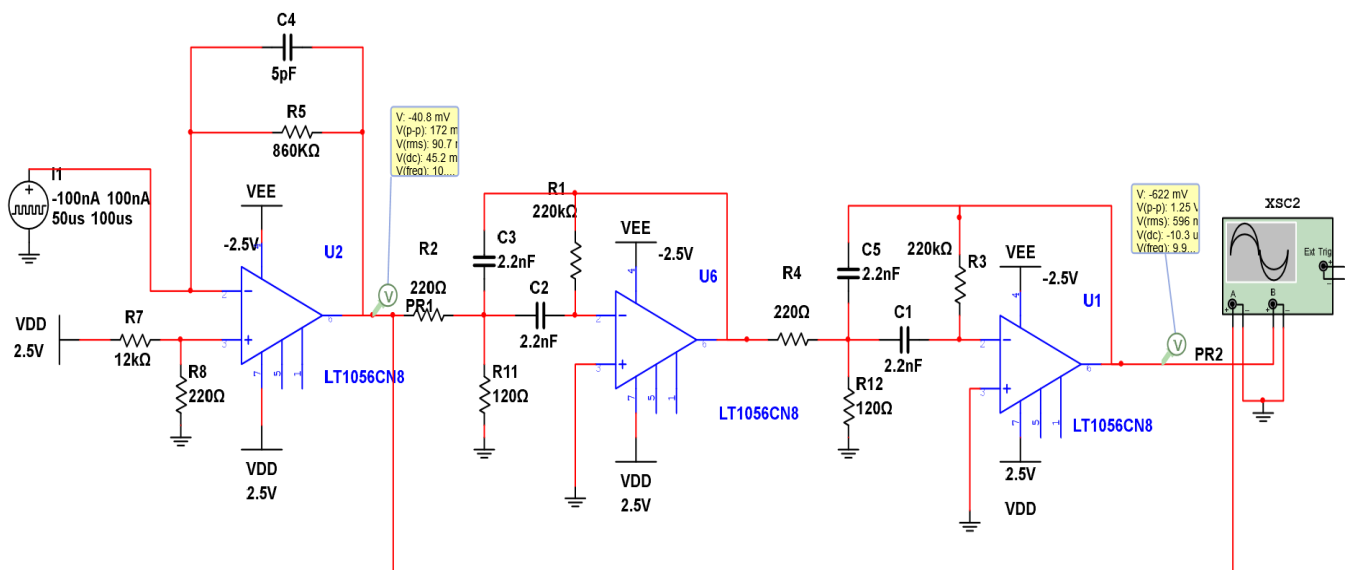
Figure 3.10 VLC receiver for resonant frequency of 10 kHz
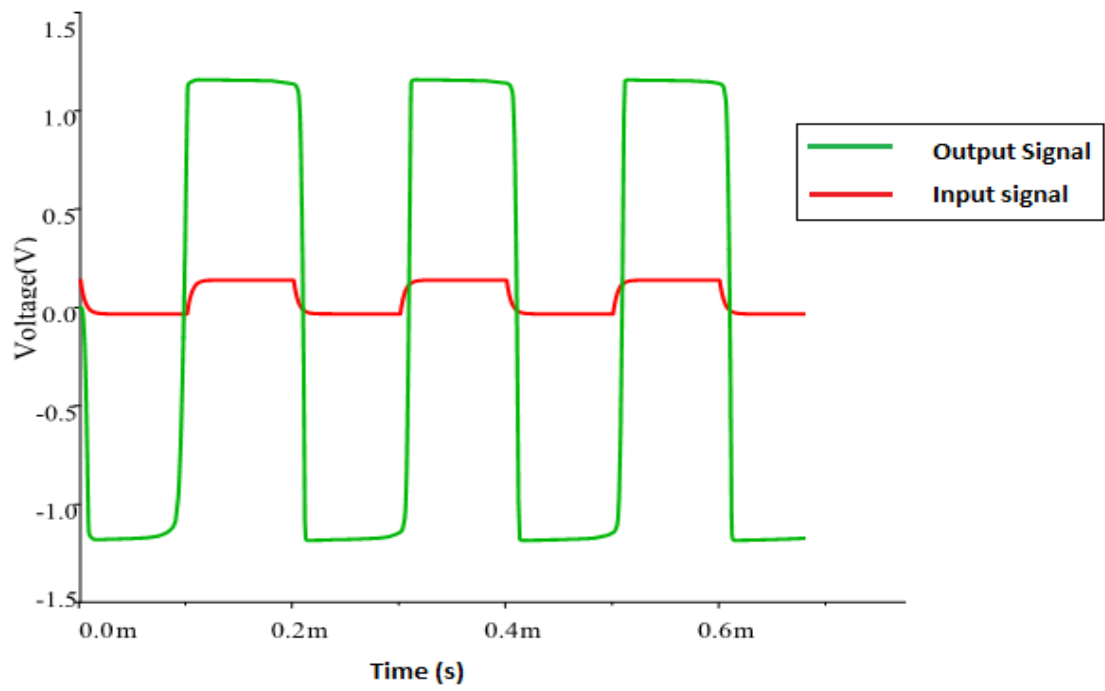
Figure 3.11 VLC receiver transient simulation fm=5 kHz
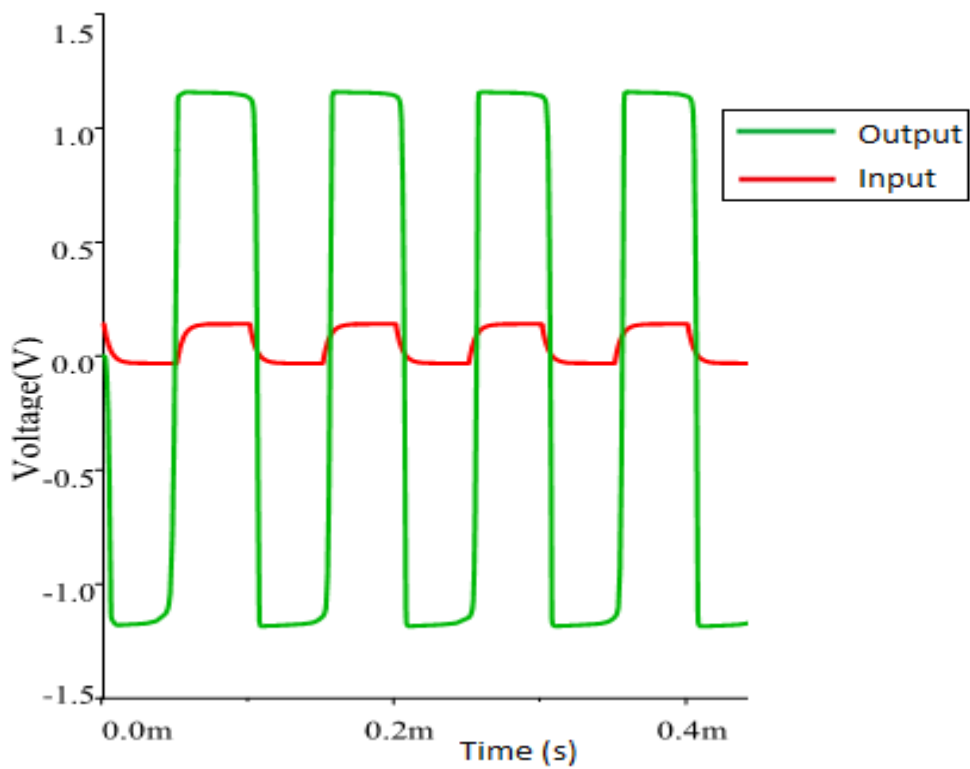
Figure 3.12 VLC receiver transient simulation fm=10 kHz

Figures 3.11 & 3.12 show the transient simulation results for 5kHz and 10kHz designs respectively. In both figures, the red cursor indicates the TIA output and the green cursor indicates the MFB filter output. It can be clearly seen that the TIA output signal is distorted due to the rise time caused by setting RC time constant, which is given by:

$$\tau = RC = (860k).(5pF) = 4.3\mu s \tag{3.5}$$

However, the signal is recovered after being passed through the 4th order MFB band pass filter.

3.4.5. Design Considerations

The MFB filter stage is able to achieve very high gain at the specified centre frequency but this comes at the price of Op-Amp noise. There are some points, which need to be taken in consideration while choosing the suitable Op-Amp for the MFB band pass filter application. First: The closed-loop bandwidth of the amplifier must be at least 100 times higher than the cut-off frequency of the filter. After defining the cut-off, frequency and selecting suitable amplifier bandwidth then the Gain bandwidth product (GBWP) of the chosen amplifier should comply with the following equation for the MFB topology and to avoid oscillation.

$$GBWP \geq 100.(-G_{CLI} + 1)f_c \tag{3.6}$$

Where G_{CLI} is inverting gain of the closed loop system and f_c is the cut-off frequency. The second point which needs paying attention is the amplifier Slew Rate (SR). The amplifier Slew rate depends on the values of the internal capacitances, resistances and currents. By choosing the appropriate amplifier SR we ensure that the filter does not create any signal distortions [48]. To achieve that the SR should be at least:

$$SR \geq (2\pi.V_{OUT\ P-P}.f_c) \tag{3.7}$$

Where $V_{OUT\ P-P}$ is the peak to peak output voltage

In the MFB topology, the Op-Amp's Input Bias current is not taken in consideration as the input capacitor C_1 blocks any input currents.

3.5. Summary

In this chapter the proposed block diagram of a tuned analog front end was explained. The standard upon which the components were chosen was also discussed. The transmitter, receiver modulation scheme and filtering stage designs were explained. Simulations were carried to evaluate the viability of the proposed system. Simulation results showed the improvements achieved by adding the filtering stage to the receiver side.

4. Experimental setup and results for VLC system using Manchester coding

In this chapter, experiments will be set to evaluate the performance of the proposed VLC system using OOK modulation and Manchester coding. Several experiments were conducted under the indoor condition and in the presence of Fluorescent lights which act as artificial ambient light noise. The performance of the system was measured through analysing the received Eye Diagram with and without the filtering stage. Two different centre frequencies were used to proof the improvement of the performance of the VLC system by applying the MFB filter. In each case Signal to Noise Ratio was evaluated for the received data at variable distances between transmitter and receiver.

4.1. VLC system using Manchester Coding implementation and results
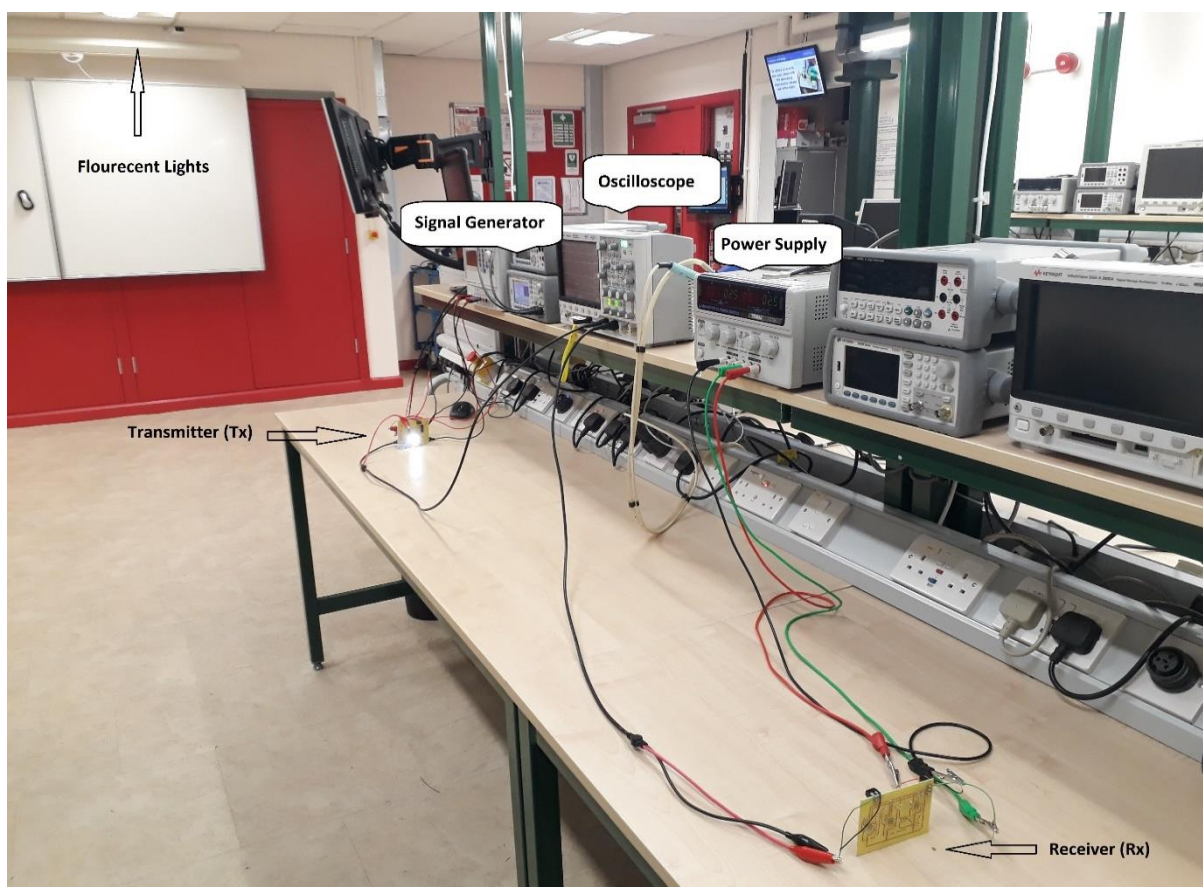

Figure 4.1 Experimental setup of VLC system using Manchester coding

Figure 4.1 shows the experimental setup of the proposed OOK based VLC system. As shown in the figure all experiments were conducted in the electronics laboratory area, which could be considered as an everyday life environment, with the availability of back ground lights interference and multipath distortion.

4.1.1. Transmitter Implementation

Based on the design previously explained in section 4.3, the transmitter circuit schematic diagram was transferred to Printed Circuit Board (PCB) using Ultiboard software tool. The 74LS86D IC was used as a digital X-Or gate to perform the Manchester encoded signal. A commercial 2N222 NPN transistor was used for the driver circuit, and a low power white light LED (Nichia 510G) was used to transmit the modulated signal.

4.1.2. Receiver Implementation

The photodiode used for receiver final implementation was VTB8440BH Silicon photodiode with infrared rejection filter for better performance under indoor conditions including different noise backgrounds. Two 10 µF electrolyte-coupling capacitors were connected across the power supply voltage rails to reduce the power supply noise detected at the oscilloscope. LT1056 Op-Amps were used in both the TIA circuit and the MFB band pass filter. The LT1056 JFET input operational amplifier combines precision specifications with high-speed performance. With a gain bandwidth product of 6.5 MHz and a slew rate of 16 V/µs makes it a suitable choice for the proposed Front-End design. A small value capacitor (5 pF) was connected in parallel with the feedback resistance of the TIA to reduce the noise. Transmitter and receiver final prototypes are shown in Appendix 2.

4.2. Results and Analysis of VLC system using Manchester coding

In this section the experimental results for the proposed OOK prototype will be analysed and discussed. The received Eye Diagram with and without filtering will be compared and the BER and SNR against distance in both cases will be evaluated.

4.2.1. Eye Diagram Analysis
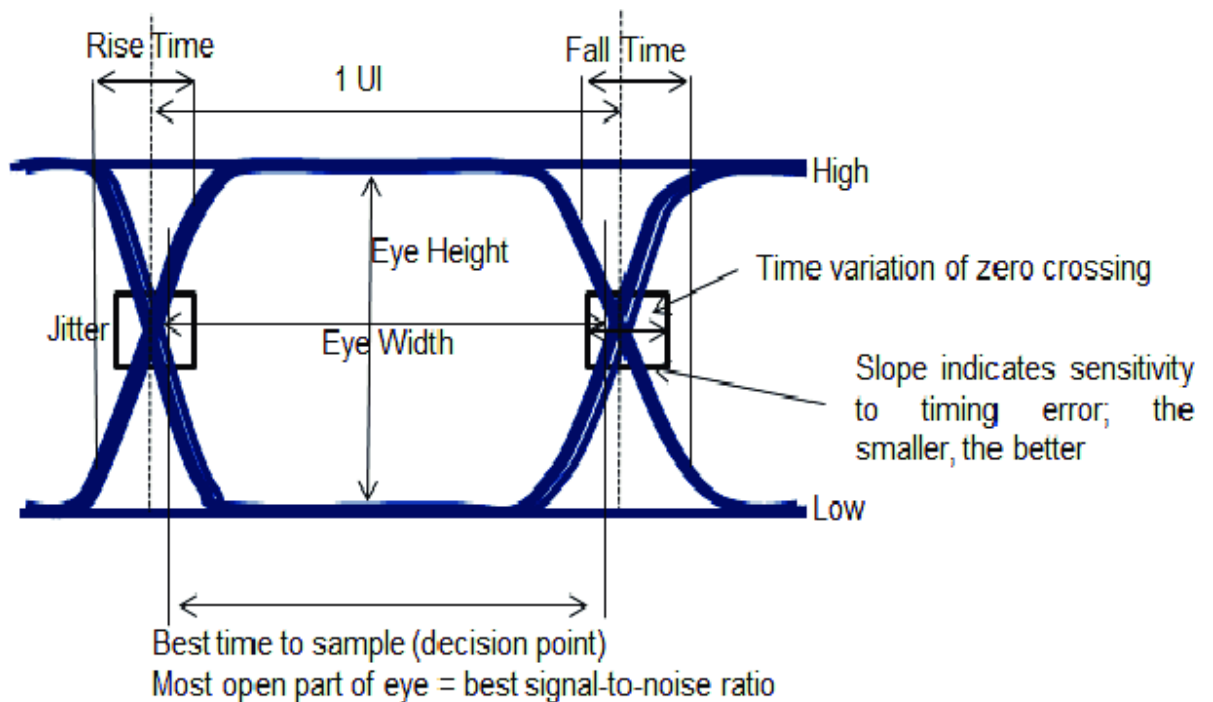
Figure 4.2 The Eye Diagram representing transmitted digital data

The Eye diagram is an oscilloscope display of a digital signal which is repetitively sampled to represent its behaviour. The Eye Pattern provides qualitative analysis for digital signal transmission and can be used to estimate the Signal to Noise Ratio (SNR), Bit Error Rate (BER) and Clock timing jitter through which digital communication systems performance could be measured [49]. In fact, the Eye pattern is the sum of a digital signal binary bits of zero's and one's corresponding transition measurements giving an image of an "eye" as shown in Figure 4.2.

4.2.2. Results for 10Kbps transmission with and without filtering

A centre frequency of 5 kHz and a transmission data rate of 10 kbps were chosen to match the MFB band pass filter receiver design. This transmission frequency band was chosen after several experiments and measurements of the MFB filter response with available laboratory components. The VLC system was set in the laboratory environment with the availability of fluorescent light lamps and several measurements were taken at different distances to compare the system performance with and without adding the filtering stage.

Figure 4.3 The Eye Diagram of Tx & Rx signals without filtering at 60 cm distance and data rate of 10 kbps
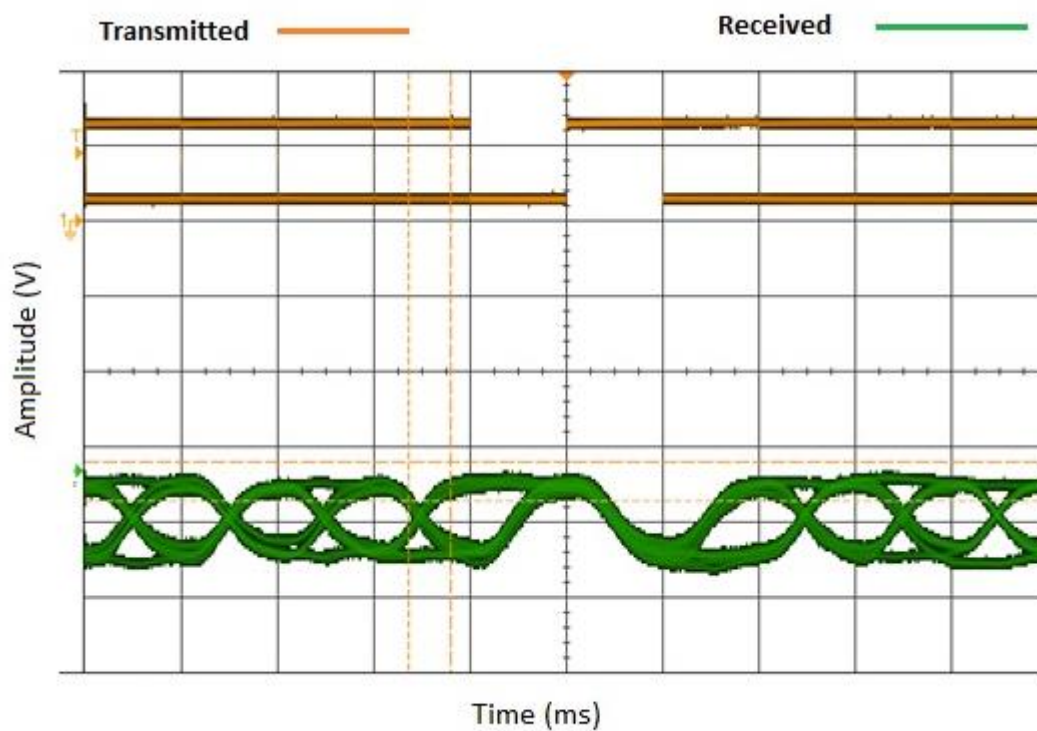
Figure 4.4 The Eye diagram of Tx & Rx signals with filtering at distance of 1.8 m data rate 10 kbps

Figure 4.3 shows the eye diagram of the transmitted and received signals of a data rate of 10 kbps without filtering and at a distance of 60 cm which is the maximum achievable distance in this case. It can be seen that received signal is distorted and covered with noi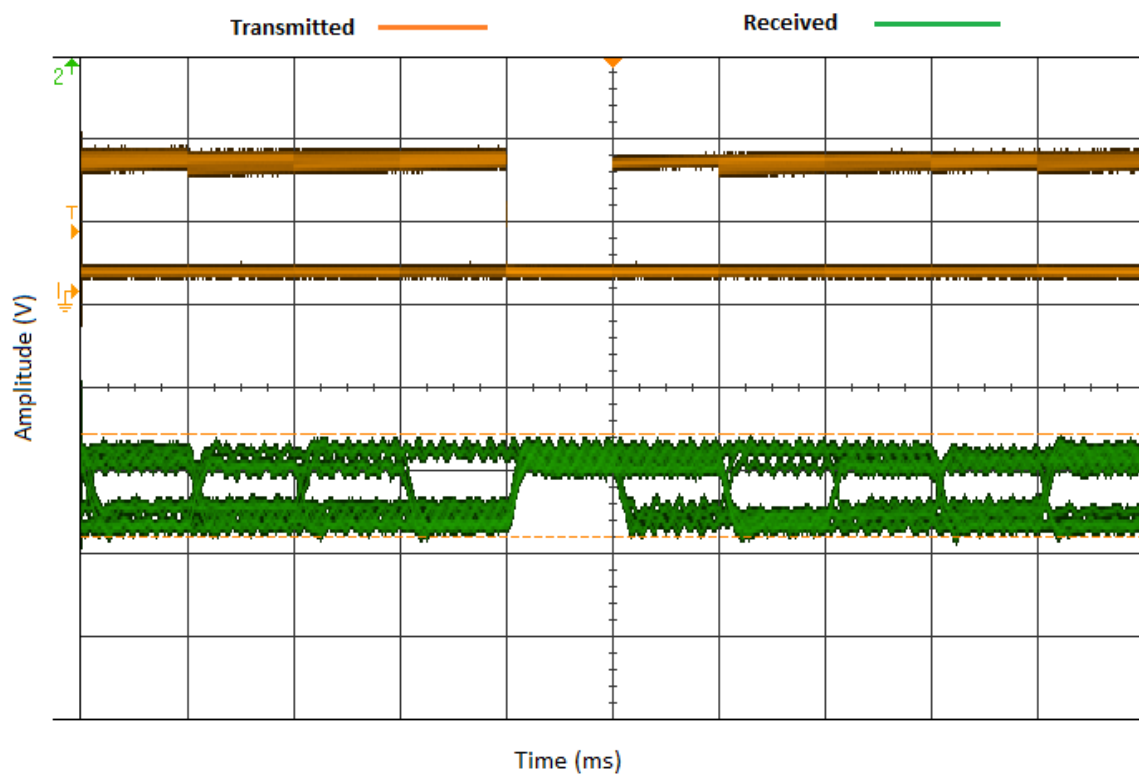se caused by fluorescent lamps. Figure 4.4 shows the eye diagrams of the transmitted and received signals at the output of the MFB filter at a distance of 1.8 m with the same data rate. From the eye diagram, it can be seen that the signal is less affected by ambient lights and can be detected up to a distance of 2.2 m.

4.2.3. Results for 20Kbps transmission with and without filtering

The same experiments were repeated for a centre frequency of 10 kHz and a transmission data rate of 20 kbps. The system performance was compared through Eye diagram analysis with and without filtering. Figures 4.5 & 4.6 show the Eye diagram of received and transmitted signals without and with filtering respectively. In Figure 4.5, the distance between the transmitter and receiver is 40cm which is the maximum achievable transmission range at this data rate. In Figure 4.6 by adding the MFB stage, the transmission range was extended to 1.6 m from the eye diagram it could be clearly seen that the system could reduce the ambient light noise caused by the Fluorescent lights in the laboratory environment.
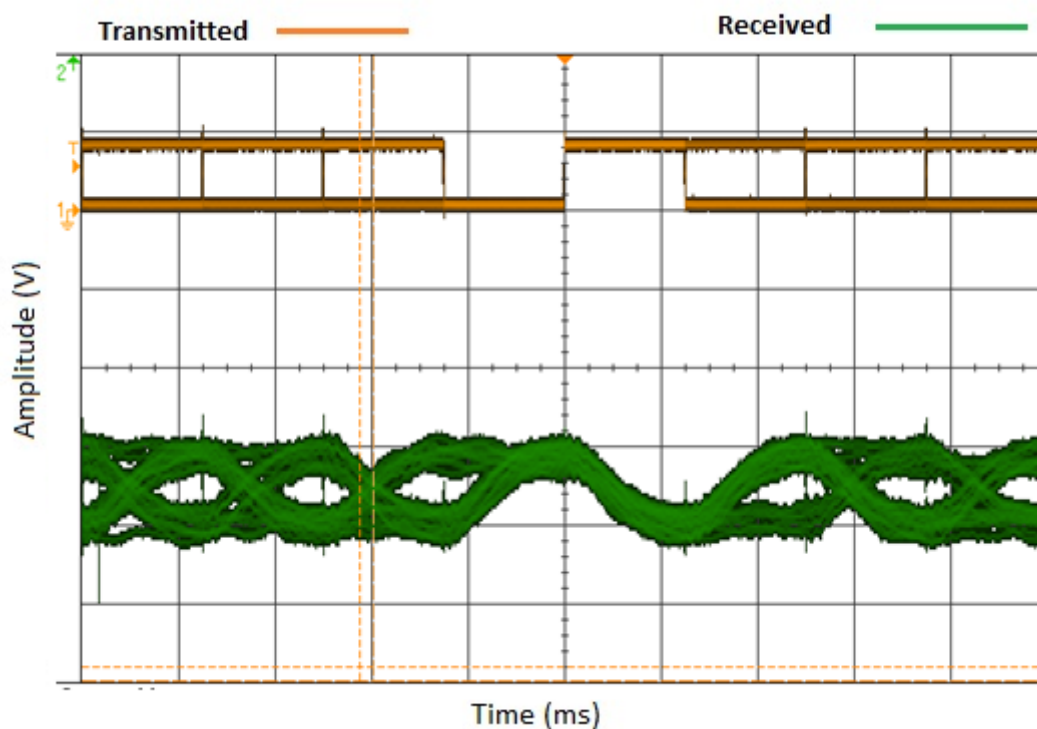
Figure 4.5 The Eye Diagram of Tx & Rx signals without filtering at 40 cm distance and data rate of 20 kbps
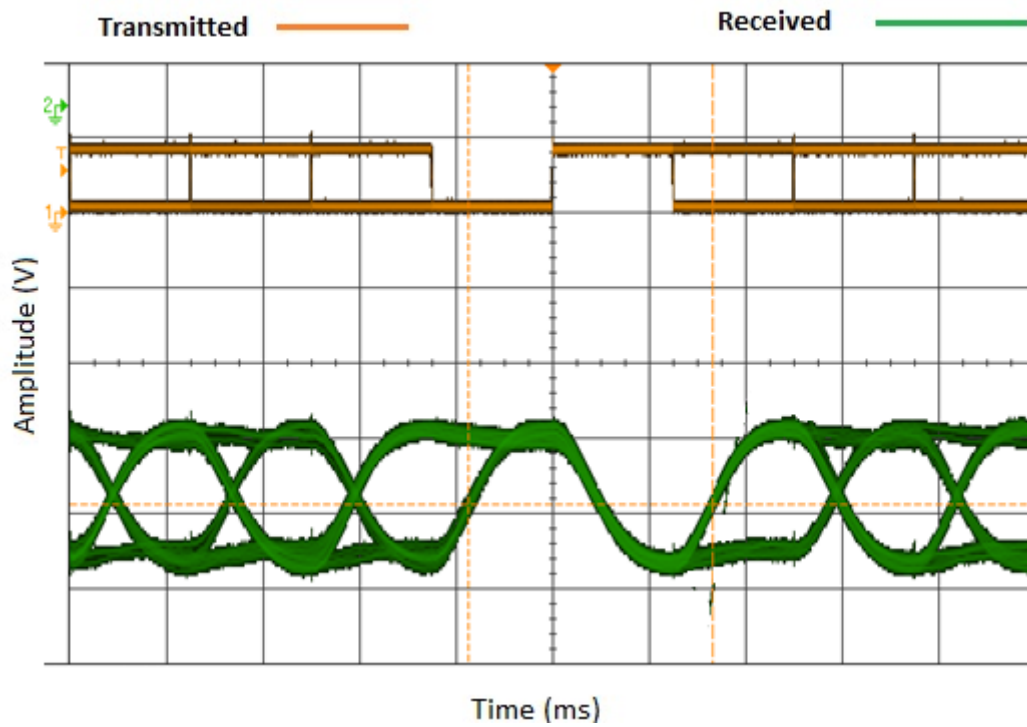
Figure 4.6 The Eye diagram of Tx & Rx signals with filtering at distance of 1.6 m data rate 20 Kbps

4.2.4.   Signal to Noise Ratio (SNR) Vs Distance

In this section, two sets of comparisons were carried out at two different resonant frequencies 5 kHz and 10 kHz. In the first case, a centre frequency of 5 kHz and a data rate of 10 kbps were used for transmission. SNR was evaluated at varied distances between the transmitter and receiver with and without filtering. Figure 4.7 shows SNR against distance plot. From the plot, we can clearly see that by employing the proposed filter the transmission range can be extended from 80 cm to 2.2 m. The same test was applied using another centre frequency of 10 kHz and a data rate of 20 kbps for transmission. From Figure 4.8 we can see that the transmission range was extended by using the proposed filter from 60 cm to 1.8 m; however, a lower data rate was achieved in this case than the previous due to the gain bandwidth product of the OP-AMP trade-off. The maximum achievable bit error rates (BER) were 2.1×10^{-12} and 4.89×10^{-10} for data rates of 10 kbps and 20 kbps respectively over a transmission distance of 1.6 m.
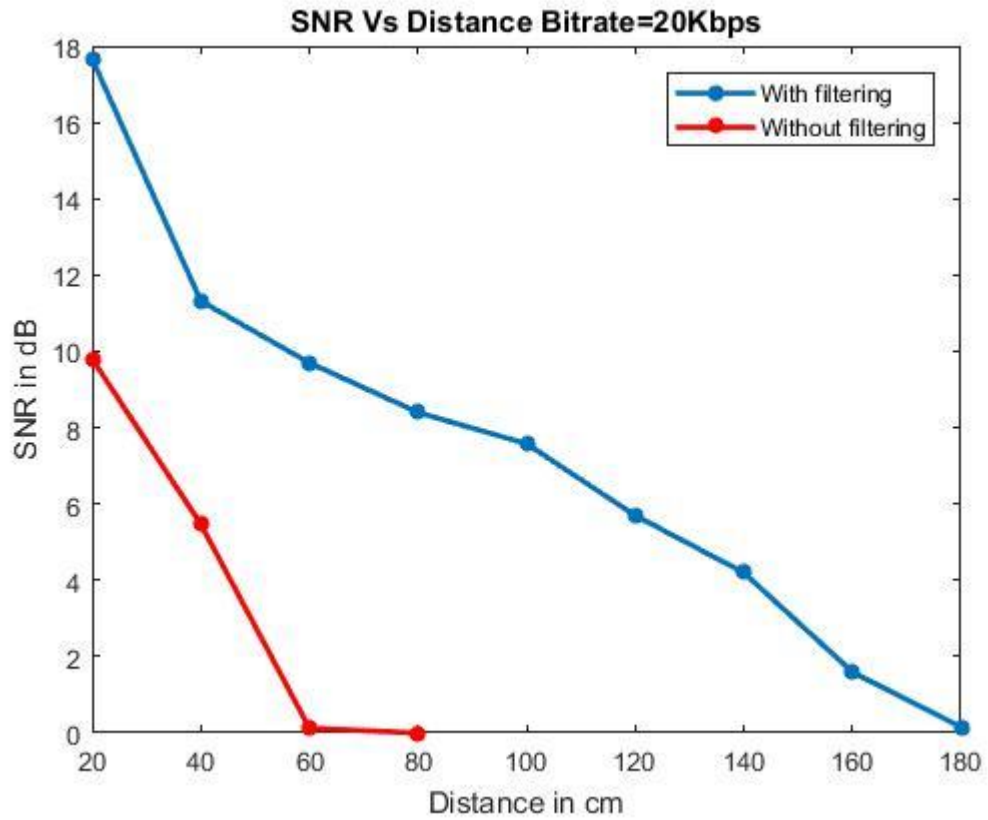
Figure 4.7 SNR against distance for fc=5kHz & data rate of 10Kbps
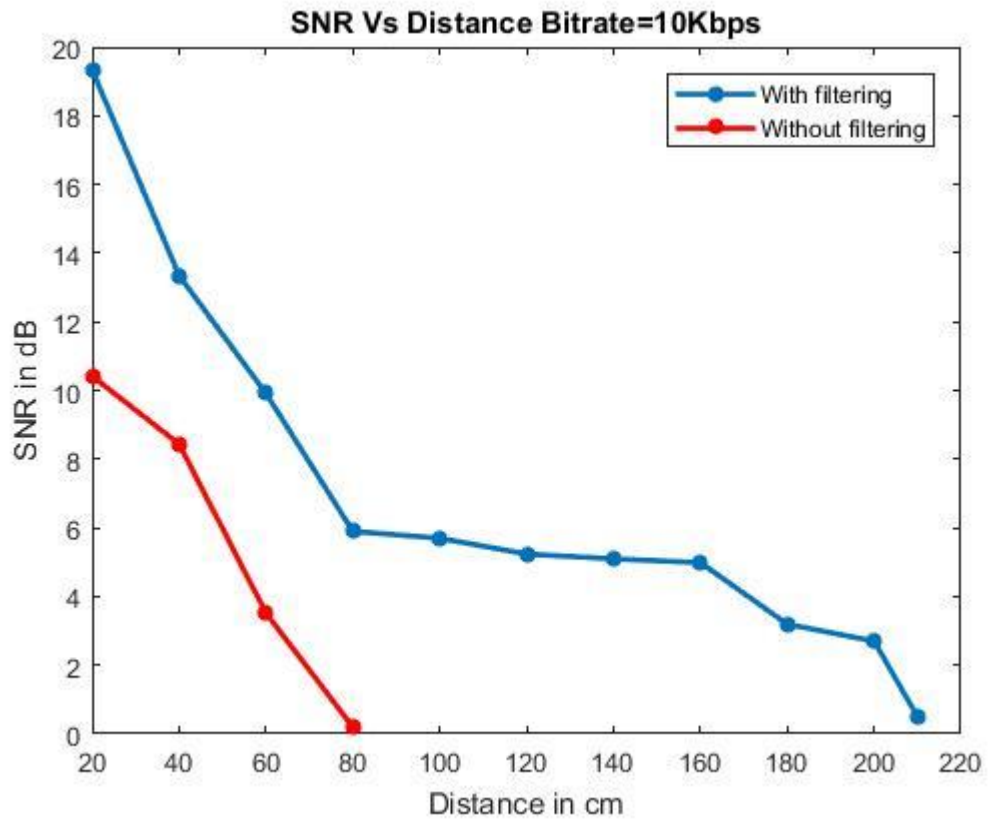
Figure 4.8 SNR against distance for fc=10kHz & data rate of 20Kbps

5. Prototype 2 Long range VLC system using PWM

PWM have been widely used in VLC systems including LED dimming control applications. By using PWM, the dimming level of the LED could be controlled without affecting the transmitted data. As the pulse amplitude is constant in PWM therefore, the spectrum of the light emitted by LED remains constant, and by the variation of the pulse width, the LED dimming level could be controlled [50]. In addition, to avoid flickering the duty ratio could be adjusted to a certain percentage without affecting the transmitted data. In some VLC applications high data rates is not required such as text delivery shopping, digital signage and running text applications. Thus, in these cases using complex and expensive modulation is wasteful. In this section, another VLC system for long-range transmission using PWM will be designed and implemented. Figure 5.1 shows the experimental setup of the VLC system based on PWM in laboratory environment. The proposed VLC system is comprised of a function generator, which generated a pulse signal of a chosen frequency. PRBS data stream is internally modulated using PWM and transmitted through the VLC transmitter driver circuit. The proposed receiver circuit detects the received signal and the captured signal is analysed by the oscilloscope.
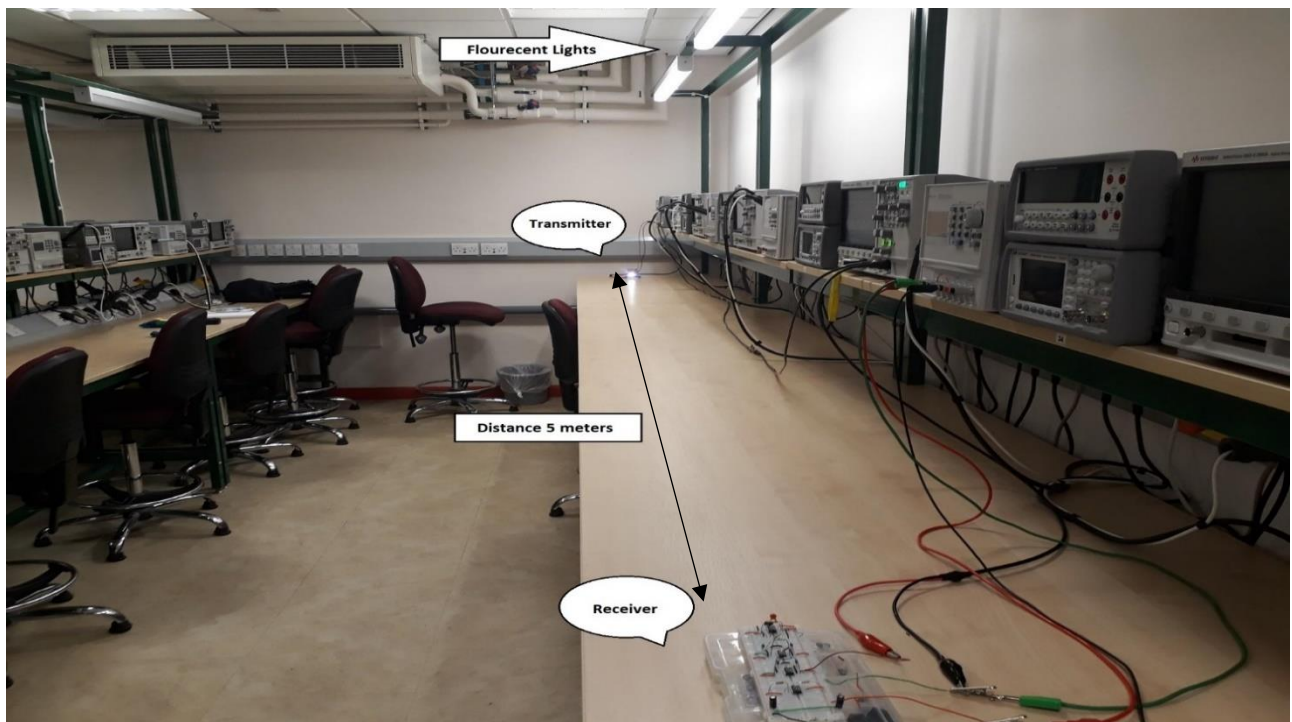
Figure 5.1 Experimental setup of long range VLC system based on PWM

5.1. LED driver circuit design and implementation

As explained previously in chapter 4 the LED driver circuit is comprised of a low power LED 0.2W driven by a common collector configuration as shown in Figure 5.2. The resistors R_1 and R_2 form a voltage divider that controls the base emitter voltage. The coupling capacitor C_1 blocks any DC signal at the input. The resistor R_3 controls the LED forward current and R_4 degenerates the emitter for early voltage improvement. The modulated PWM signal is transmitted through visible light using the low power LED.
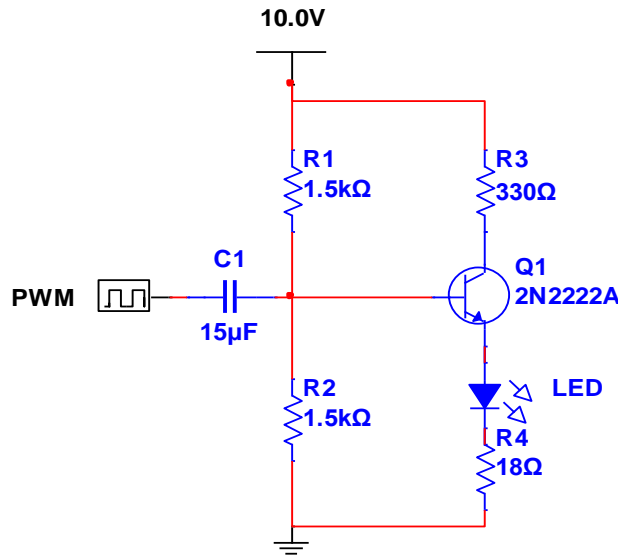
Figure 5.2 LED driver circuit design

5.2. Receiver design and implementation

The proposed receiver circuit is comprised of a photodiode, Transimpedance amplifier, 4th order multiple feedback band pass filter and a comparator. Figure 5.3 shows the proposed VLC receiver with the value of the components corresponding to each module. After being detected by the photodiode, the obtained electrical signal is fed to the TIA where the current to voltage conversion occurs. As previously explained in chapter 3 the proposed 4th order multiple feedback band pass filter operates at the defined transmission frequency allowing only the desired frequency band and rejecting unwanted frequencies including ambient light interference caused by fluorescent lamps and other lighting backgrounds within the laboratory environment. Finally, to overcome the signal distortion the signal is fed to a

comparator for recovery. The proposed receiver circuit was finalized and printed on PCB. The final receiver and transmitter circuits implemented on PCB are shown in Appendix 3.
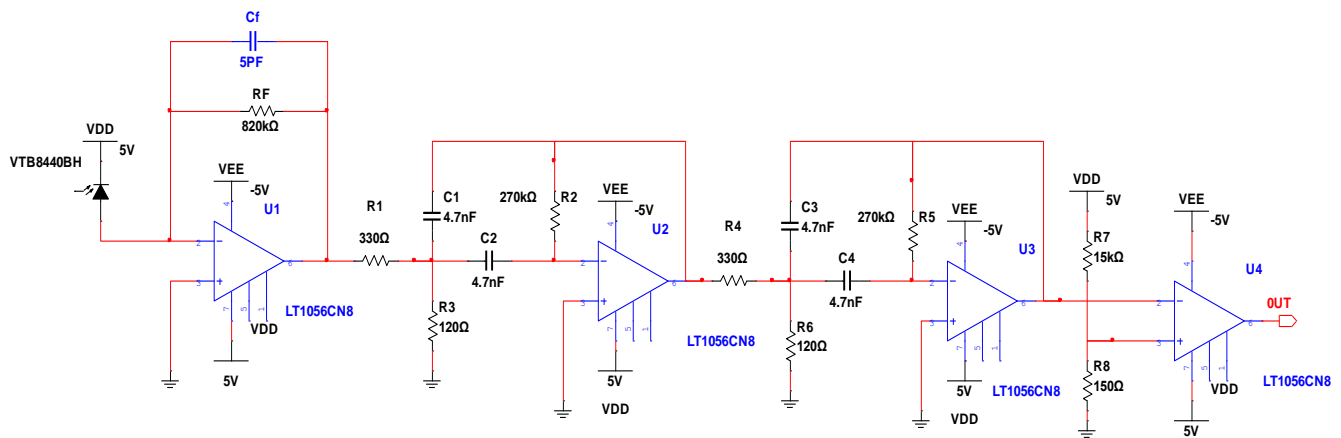
Figure 5.3 Proposed PWM receiver design

5.3.   Results and Analysis of VLC system using PWM

Experimental tests were performed to measure the performance of the proposed VLC system for the indoor condition within the laboratory environment with the availability of florescent lights and noise background. The first approach was to set the transmitter side. Using function generator, a pulse signal with frequency of 5kHz is generated. A pulse width of 100 μs and edge time of 50 ns was chosen. A PRBS signal with a bit rate of 10 Kbps was modulated using PWM and width deviation of 20 μs. In the receiver side, the MFB band pass filter is designed to operate at the transmission frequency which is 5 kHz.

5.3.1.   System improvement by employing the MFB band pass filtering stage

To measure the efficiency of the proposed receiver the pulse shape of the signal captured by the oscilloscope is observed and compared to the transmitted signal with and without the filtering stage at varied distances. The comparator is then adjusted to the required threshold voltage at the maximum achievable distance to correct the pulse shape. Figure 5.4 shows the received signal at the output of the TIA without filtering at distances of 1.5 m, the effect of noise caused by ambient light on the received pulse could be clearly seen, in addition the receiver detection range is limited to 1.5 m and further than this distance no signal can be detected. To measure the improvement achieved by adding the filtering stage the received

signal is observed at varied distances and signal to noise ratio is evaluated with and without filtering. Figure 5.5 shows the received signal at the distance of 4.5 m. The improvement in transmission range and noise immunity could be seen by observing the received signals.

Figure 5.4 TIA output signal without filtering distance of 1.5m
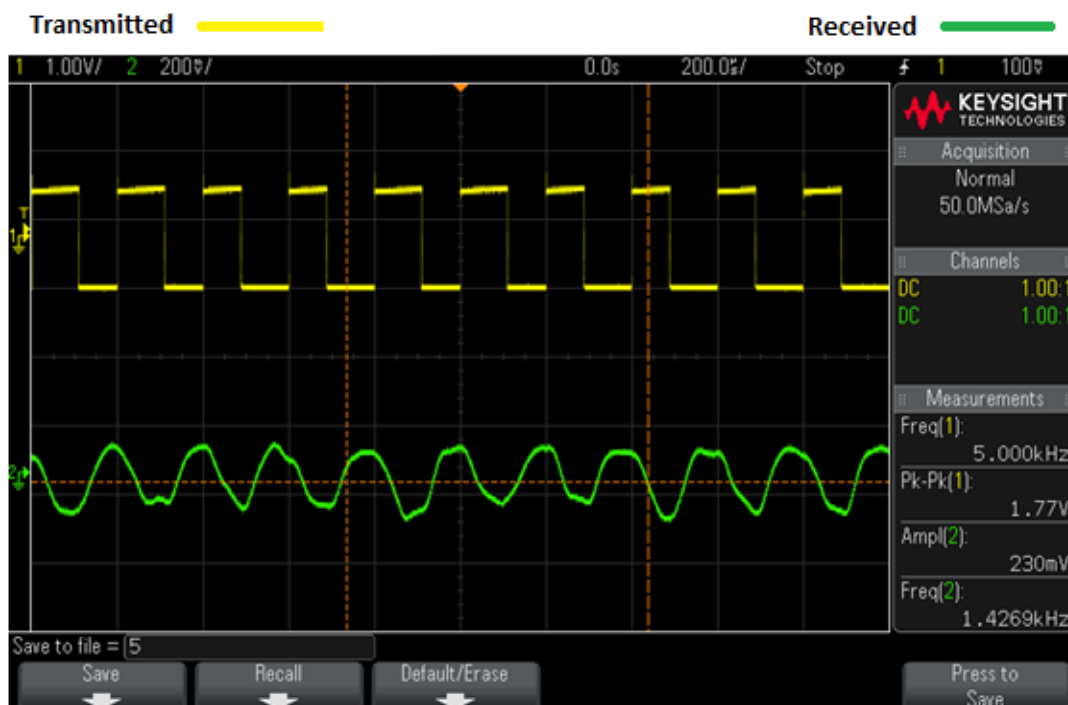
Figure 5.5 MFB output signal distance of 4.5m
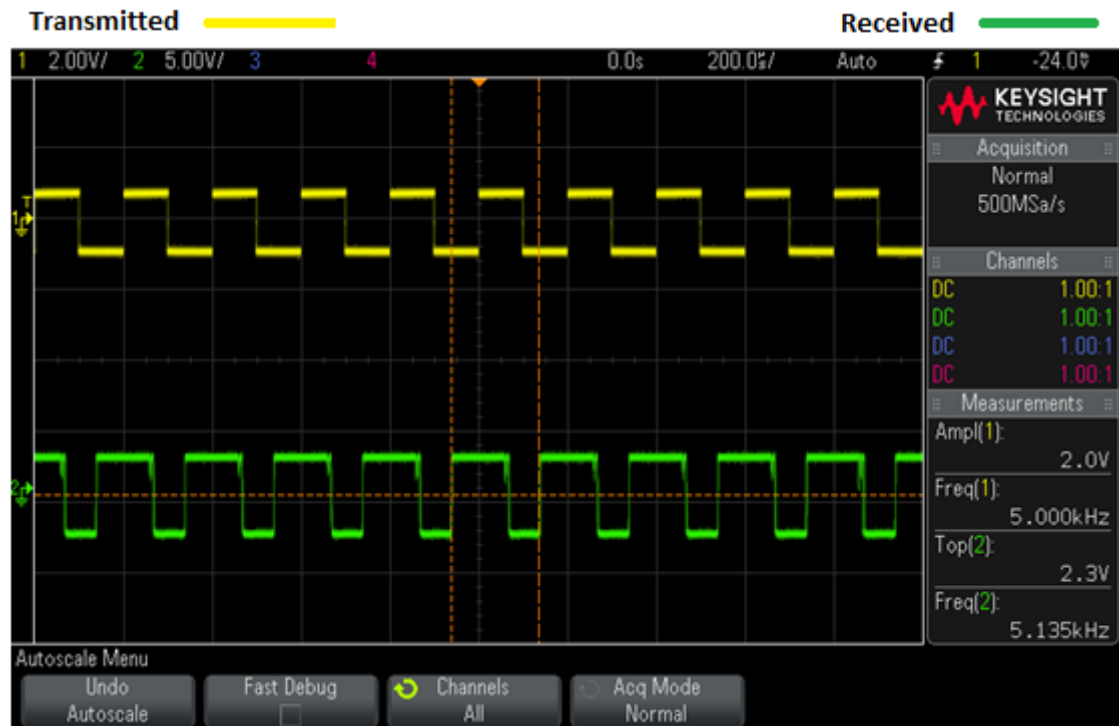
Figure 5.6 Output signal of comparator at distance of 4.5m

To overcome the distortion in the received waveform the signal is passed through a comparator. Figure 5.6 shows the transmitted and received signals after being corrected by the comparator. From Figure 5.6 it can be seen that the received signal is identical to the transmitted signal however, there is a slight compensation of delay between them of an amount of 100-500 μs, which can be ignored.

5.3.2. Signal to Noise Ratio (SNR) Vs Distance

To proof the improvement achieved by employing the proposed MFB band pass filter stage the signal to noise ratio at the output of the MFB stage is evaluated at different distances with and without employing the filtering stage. Figure 5.7 shows the signal to noise ratio against distance with and without filtering. From the plot we can see that at a distance of 2 meters from the transmitter without filtering, the SNR drops below 1 dB which means That the noise level is higher than the signal power and the signal cannot be detected. However, by employing the proposed MFB filtering stage a SNR of above 5 dB is achieved at a distance of 3.5 m from the transmitter and up to a distance of 4.5 m the signal con still be detected . By

comparing SNR in both cases, we can clearly see that there is significant improvement in SNR over distance with the MFB filtering stage
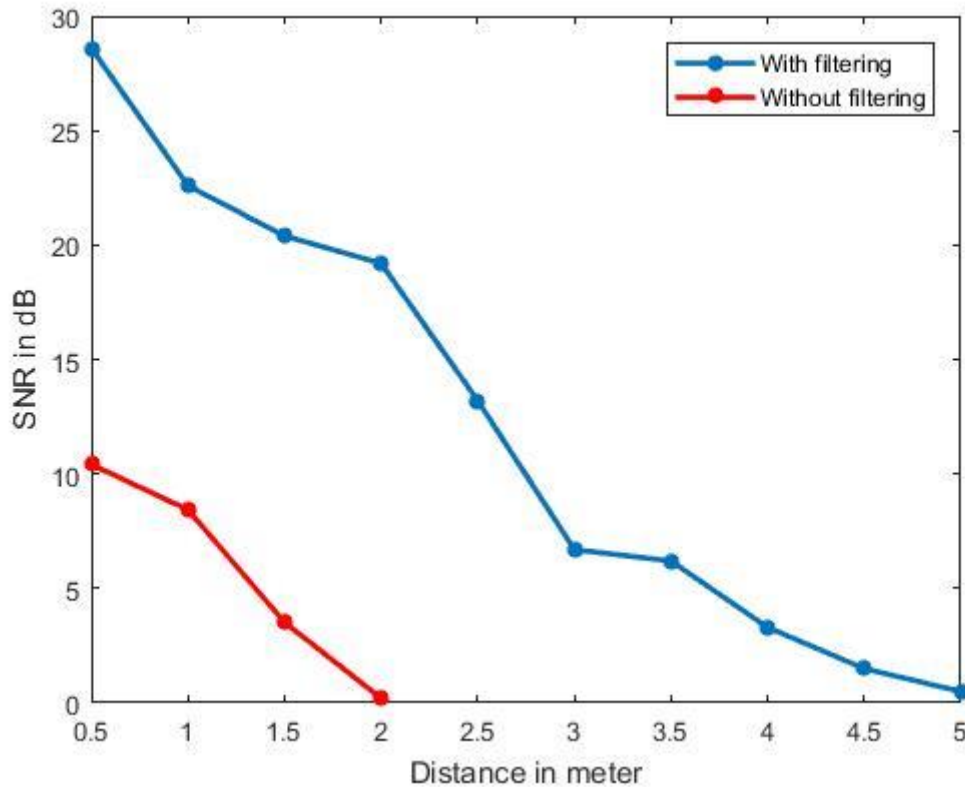
Figure 5.7 SNR against Distance PWM VLC link

5.4. Summary

Through this chapter the proposed prototypes were experimentally tested in the laboratory. In the first experiment Manchester coding modulation was used. A brief explanation of the transmitter and receiver implementation was given. Experimental results were analysed by comparing the received eye diagrams with and without the filtering stage. SNR and BER were evaluated from eye diagram measurements at variable distances from the transmitter. Results showed that by adding the filtering stage the transmission link could be extended from 40 cm to 2 m using this method. The second experiment was carried using PWM. A brief description of the transmitter and receiver sides designs was given. Experimental results showed that by using this method the VLC transmission link can be extended from 1.5 m to 4.5 m with a noticeable improvement in noise immunity.

6. Arduino Prototype

After development and implementation of VLC system and testing its performance in laboratory by sending signals generated using a function generator and observing the output through an oscilloscope, in this chapter an Arduino prototype will be implemented to test the ability of the VLC system to transmit text data. Figure 6.1 shows the block diagram of the VLC system using Arduino Microcontrollers. The ATmega328p (Arduino Uno) microcontroller was chosen due to its cheap price and reliability for low speed serial data communication. In the following sections, the transmitter and receiver designs and obtained results will be explained. Before practical implementation, the system was simulated using Autodesk Circuits simulation tool.
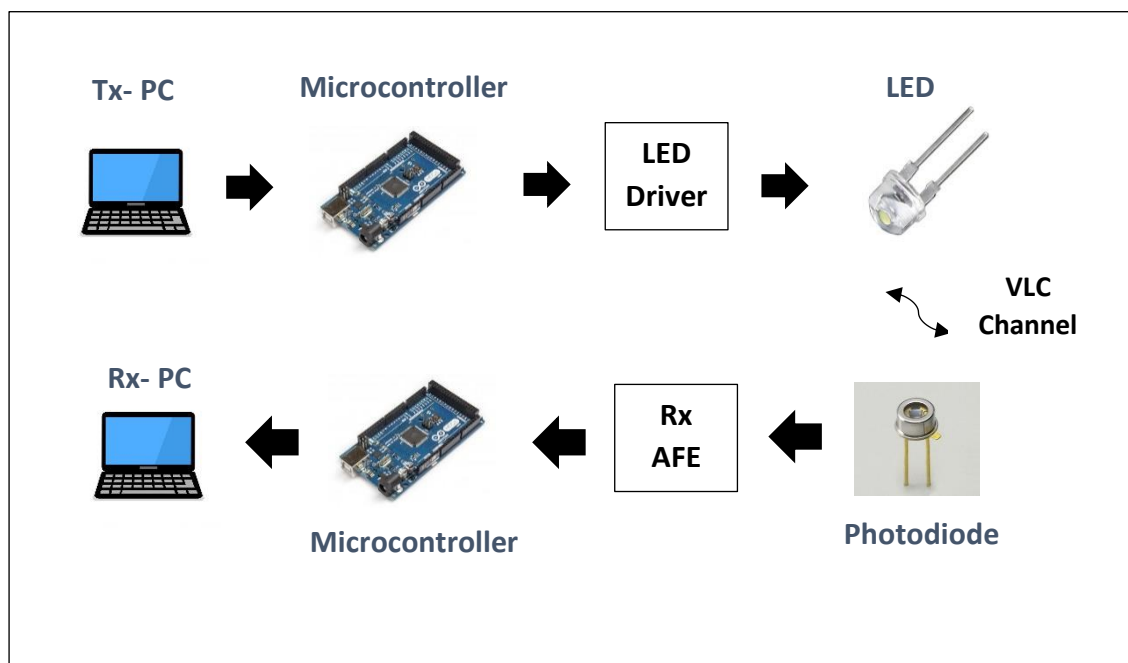
Figure 6.1 Block diagram of proposed VLC system for indoor text data transmission

6.1. Arduino Transmitter Design

The transmitter design comprises of an Arduino Uno Microcontroller board connected to the transmitting PC (PC-Tx) via USB cable, which provides power supply in addition to data interface. As previously explained in section 4.3.2. The LED driver circuit is formed of an NPN transistor with a common collector configuration. The data stream sent by PC-Tx will be encoded using PWM modulation and transmitted through the white light LED. Figure 6.2 show the schematic diagram of the VLC transmitter designed using Autodesk Eagle simulation tool. Digital Pin 4 was used as an output pin through which the encoded data will be fed to the LED driver circuit and therefore transmitted in light medium.
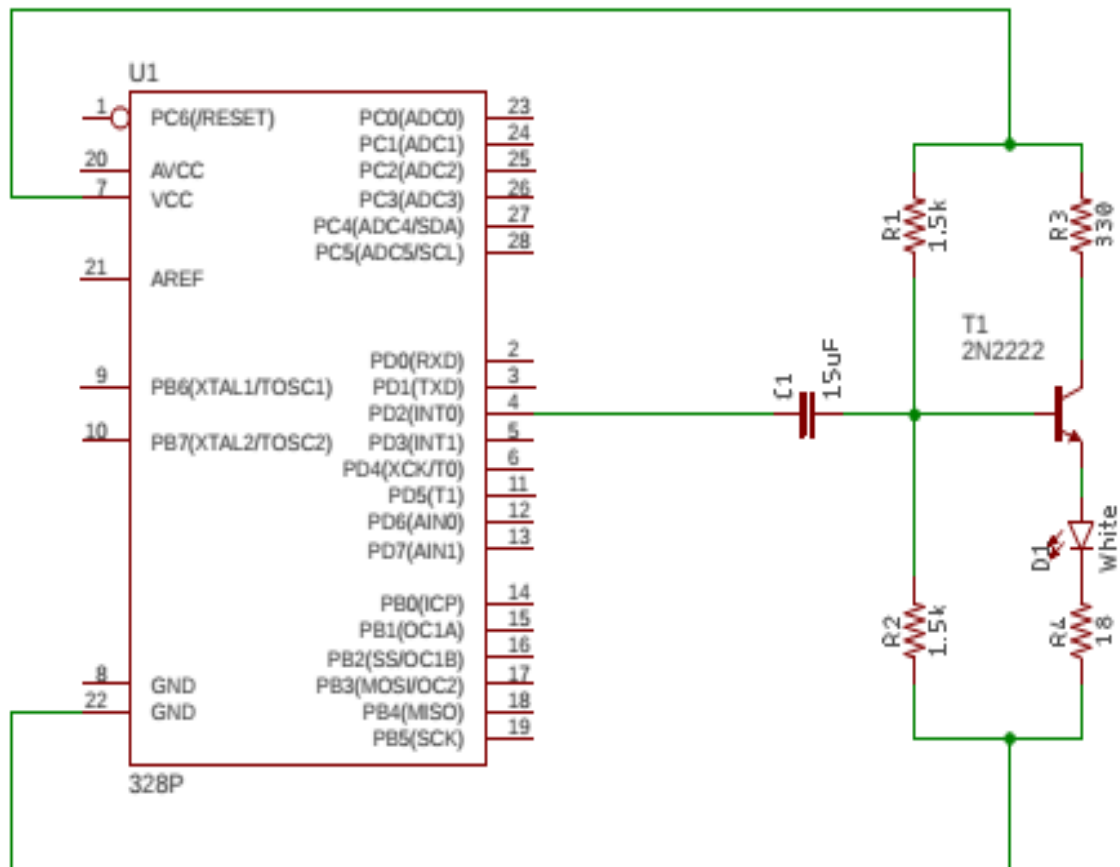
Figure 6.2 Schematic diagram of the Arduino VLC Transmitter

Before implementing the transmitter in laboratory practically the proposed circuit was simulated using Autodesk Circuits simulation tool. Figure 6.3 show the VLC transmitter simulation using Autodesk Circuits. The data stream fed to the LED to be transmitted through light can be seen through the virtual oscilloscope.
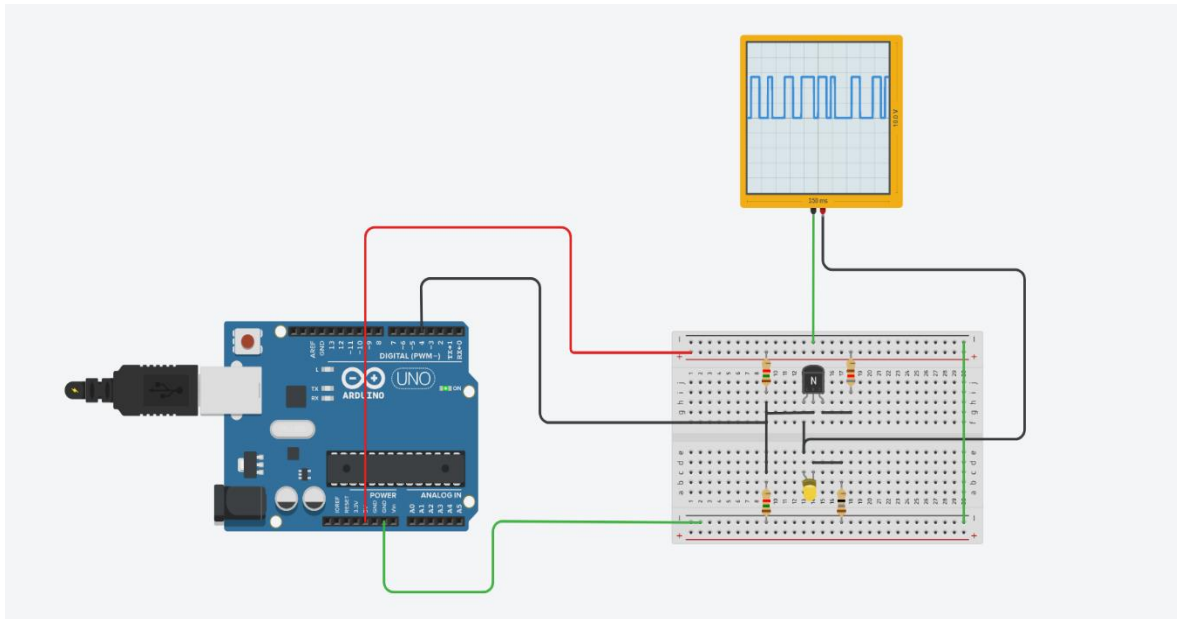
Figure 6.3 Simulation of VLC Transmitter using Autodesk Circuits

6.1.1. Algorithm for encoding data and transmission

In this section, the algorithm followed for modulation and transmission will be explained. First, each character will be given a 7-bit binary code similar to the American Standard Code for Information Interchange (ASCII). Then, this binary code is transmitted from the Most Significant Bit (MSB) to the Least Significant Bit (LSB) by turning the LED ON for every binary "1", and OFF for each binary "0". Through this procedure, VLC takes place. Figure 6.4 shows the flowchart followed during the microcontroller transmission.
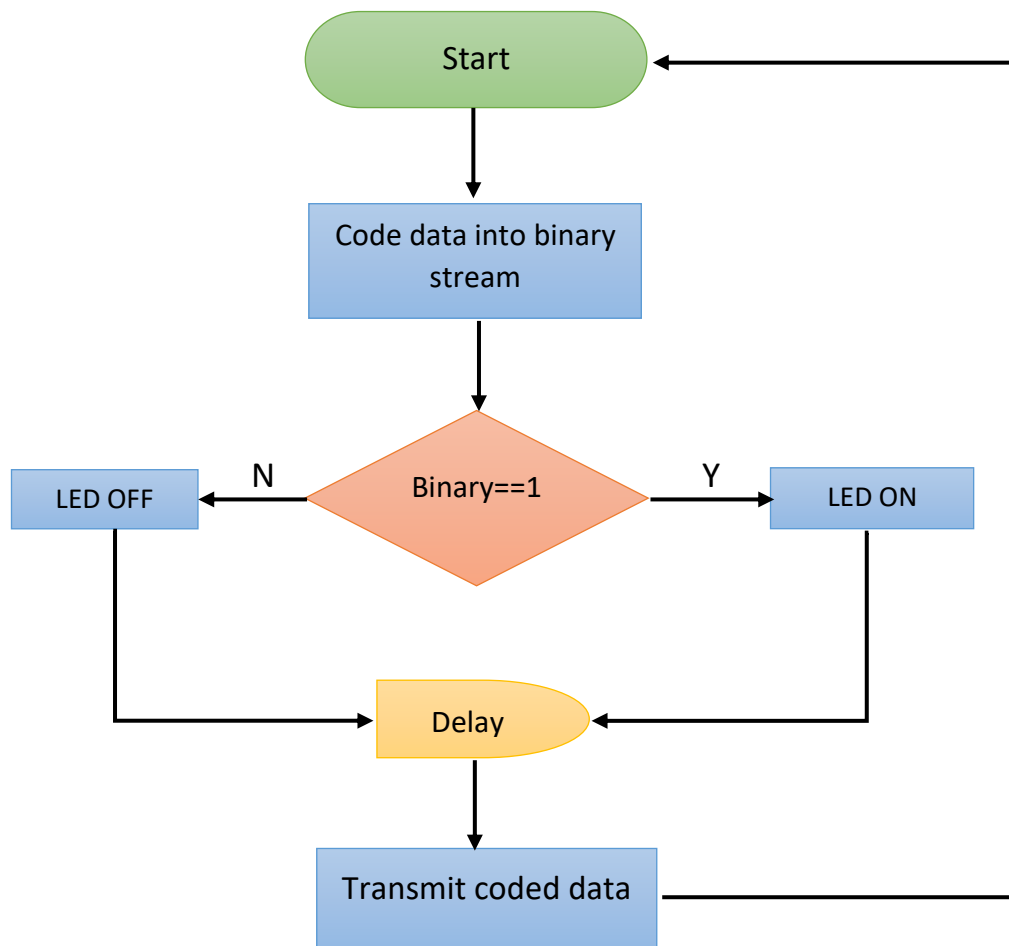
Figure 6.4 Flowchart of the Microcontroller transmitter

6.2. Arduino Receiver Design

As previously explained in section 5.2 The receiver circuit consists of a photodiode, Transimpedance amplifier, and fourth order multiple feedback band pass filter and a comparator. The ATmega328P microcontroller is added to the receiver circuit for demodulation.
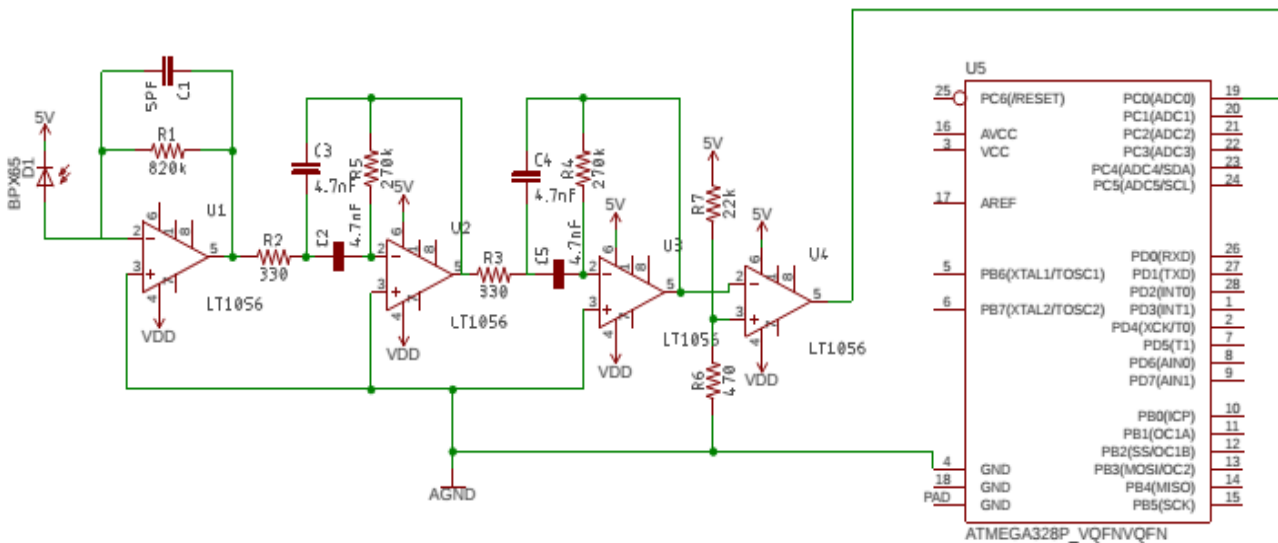
Figure 6.5 Schematic diagram of the Arduino VLC Receiver

Figure 6.5 shows the schematic diagram of the VLC receiver designed using Eagle Autodesk software tool. As shown in schematic the output of the comparator is connected to the Analog pin A0, while the ground pin is connected to the circuit ground.

6.2.1. Algorithm for receiving and decoding data

In the receiver code, a fixed integer will be assigned to calibrate the receiver's sensitivity depending on the transmission distance. This fixed integer will be given as the voltage threshold level over which the code will distinguish between logic "1" and logic "0". By setting this threshold level, the receiver is calibrated with the DC level over which the signal is received. The next step is comparing the received binary stream with the allocated voltage threshold level, and therefore reading the binary data from MSB to LSB and storing the result in a buffer. Follows that the decoding procedure, where the binary data is converted to characters which will be displayed on the serial monitor of the receiver PC. An additional case for error detection was added to the code to display an error message whenever unexpected characters are received, and through this process, an estimation of data loss was evaluated. Figure 6.6 shows the flowchart followed by the microcontroller receiver.
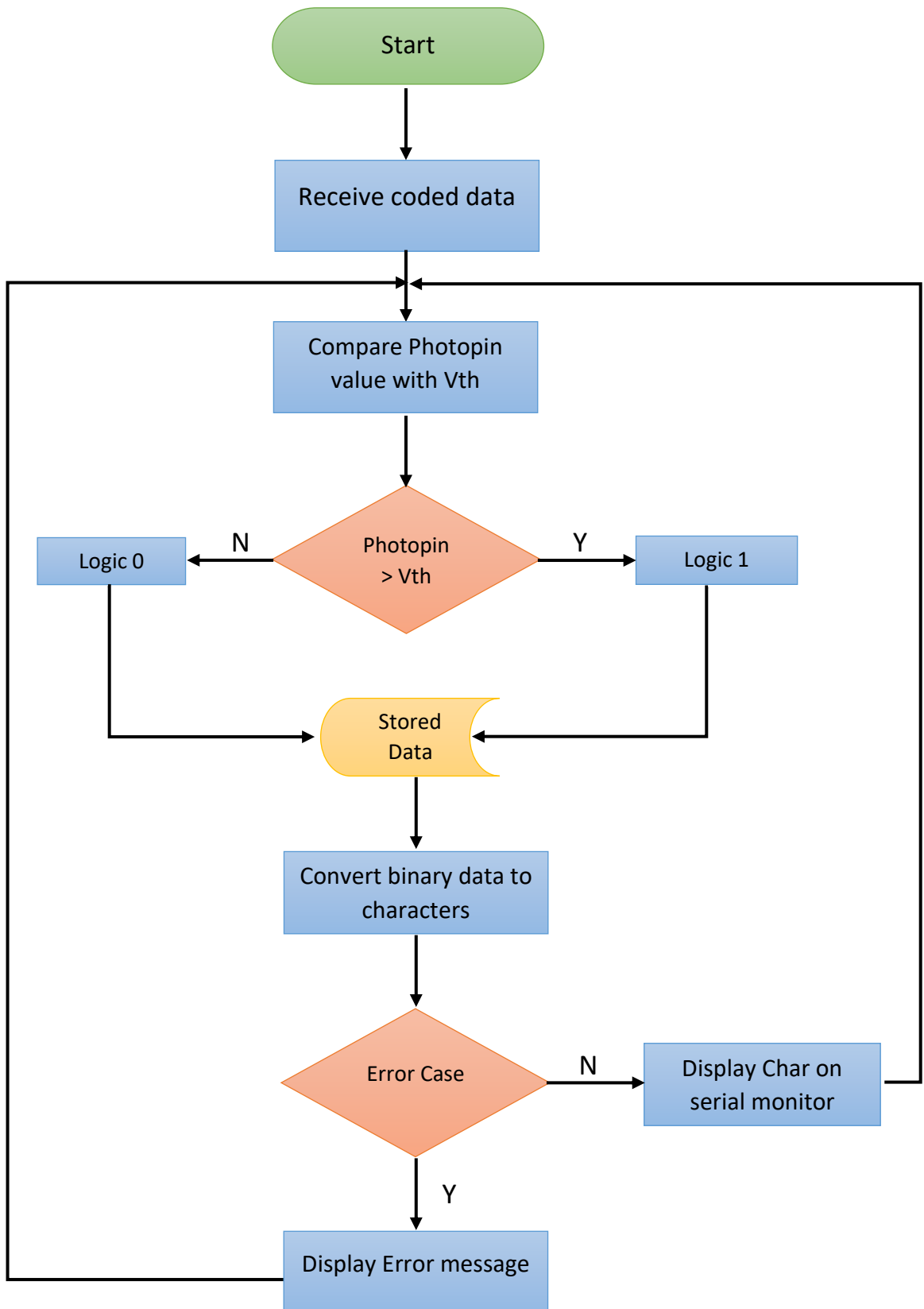
Figure 6.6 Flowchart of the Microcontroller receiver

6.3.   Arduino Prototype Experimental Setup and Results
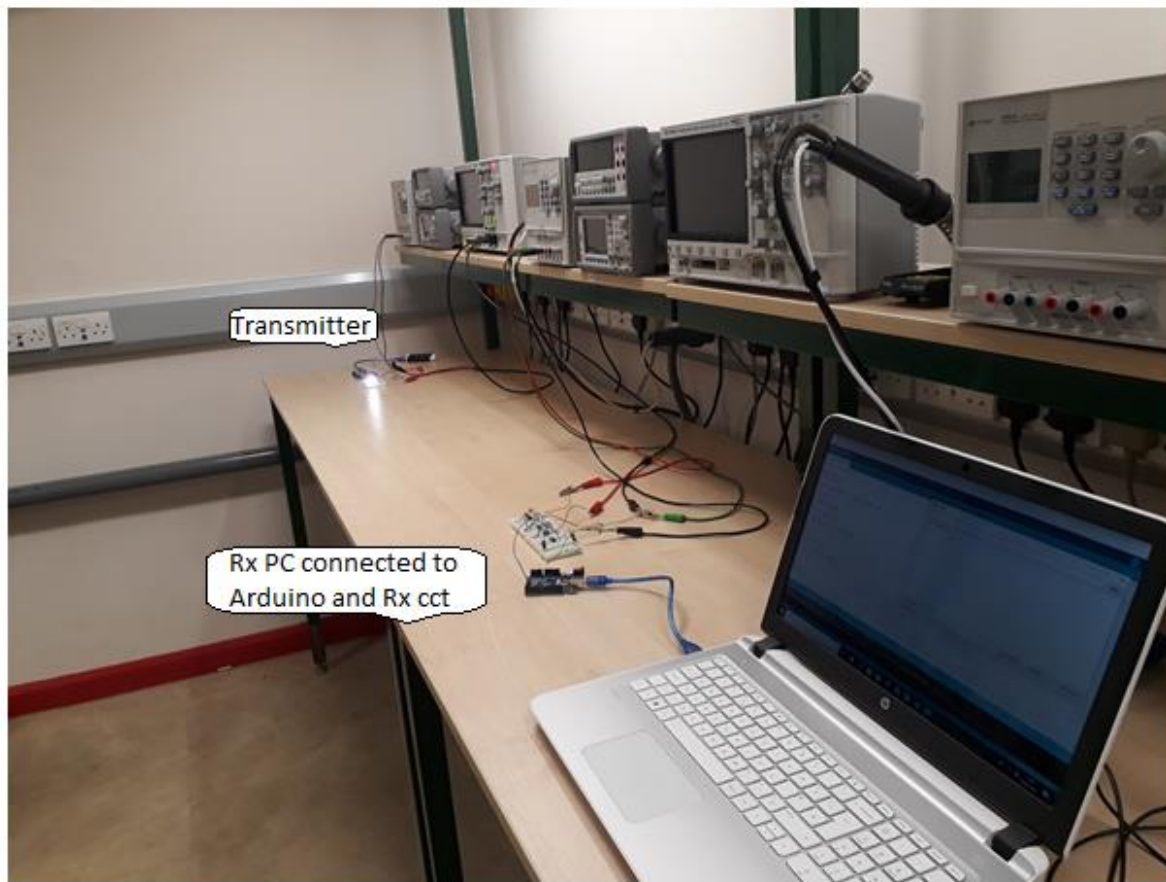
Figure 6.7 Experimental setup of Arduino VLC system in laboratory

Figure 6.7 shows the experimental setup for the Arduino VLC system in the laboratory environment. In this experiment two ATmega328P microcontroller mounted on Arduino Uno, boards were used. One PC connected to the receiver board through USB cable interface to read the detected signal on the Arduino serial monitor, while the Transmitter Arduino board was uploaded with its code to continuously transmit a the sequence of letters ("a,b,c,d") followed by the binary code for each letter. The transmitting sketch is saved to the Tx Board and a power bank supply is connected to it rather than using two PCs for the experiment. The Tx-board is connected to the LED driver circuit to transmit the encoded signal through the white light LED. The receiver board is connected to the receiver Analog Front-end to decode the received signal and display the output on the PC serial monitor. Both input and output signals were also observed using the oscilloscope. The distance between the transmitter and receiver was varied and the voltage level of the detected signal measured at each distance.

According to the voltage level, the threshold integer in the receiver code is modified to enable the microcontroller to distinguish between "1" and "0". Figure 6.8 shows transmitted and received signal at the output of TIA at a distance of 0.5 m. From figure we can observe the noise on top of the signal caused by ambient light background in the laboratory, also the transmission range is limited to 0.5 m. Figures 6.9 and 6.10 show the received signal captured at the outputs of the MFB filter and the comparator respectively at a transmission distance of 150 cm. Due to the RC characteristics of the filter the received signal at the output of the MFB filter suffers from distortion and obviously is inverted therefore, cannot be demodulated by the Rx-microcontroller. The comparator at the final stage inverts the signal and corrects the distortion caused by the previous stage. Figures 6.11 and 6.12 show the received data displayed at the serial monitor of the receiver PC. When the transmitter is shielded, no more data is received and 0's are displayed on the monitor. The Tx and Rx are not precisely synchronised in other words, the transmission and reception does not occur at the same time, due to that several errors were detected.
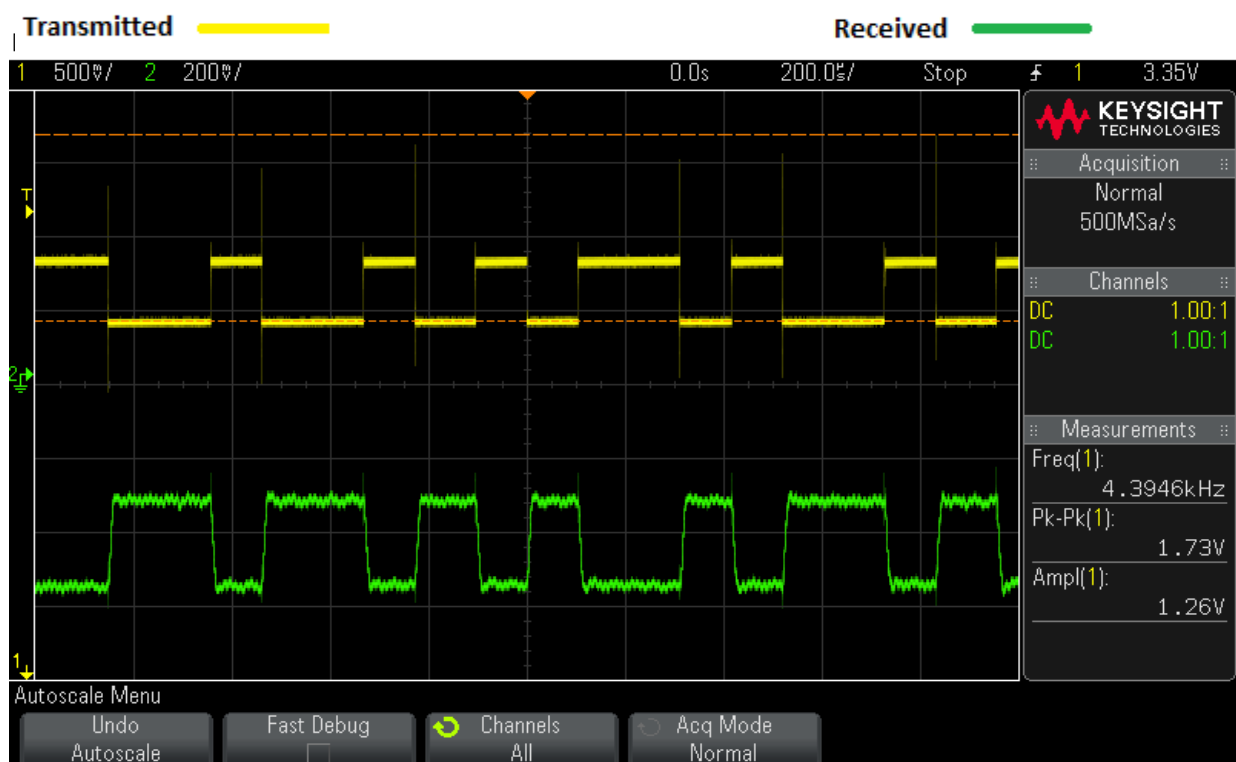
Figure 6.8 Signal captured at the output of TIA distance of 50cm

Figure 6.9 Signal captured at the output of MFB filter distance of 150cm
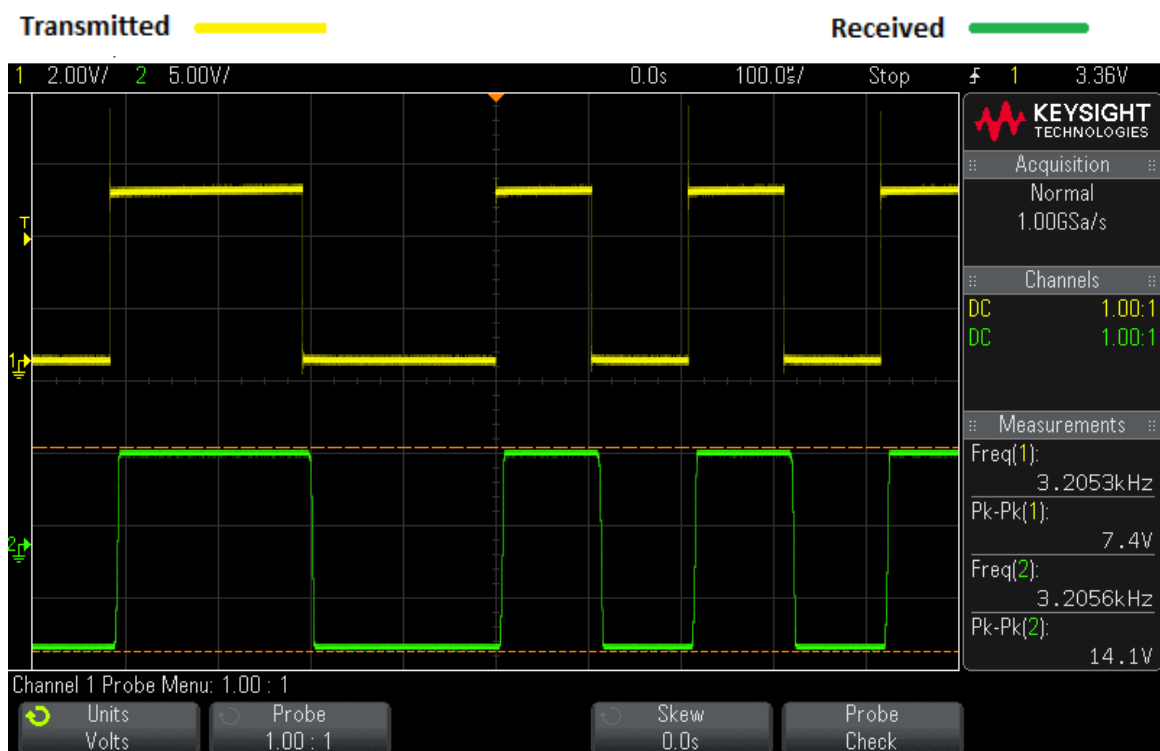
Figure 6.10 Signal captured at the output of the comparator distance of 150cm
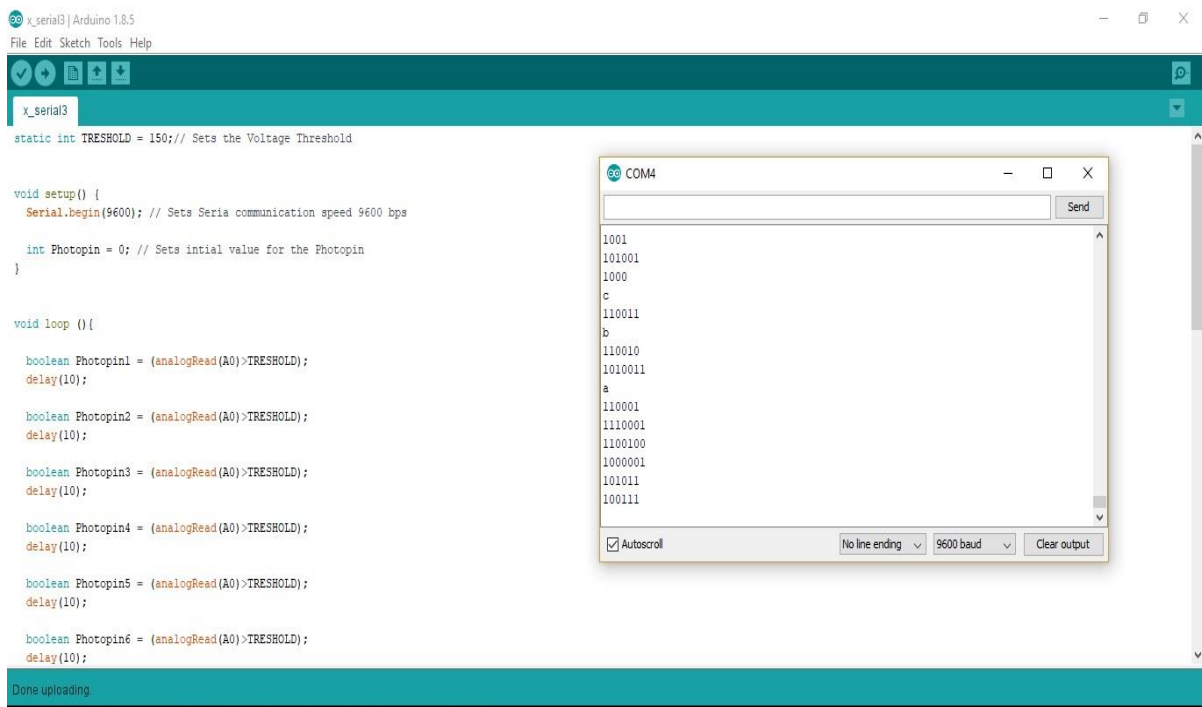
Figure 6.11 Received data displayed at the Rx-Pc serial monitor
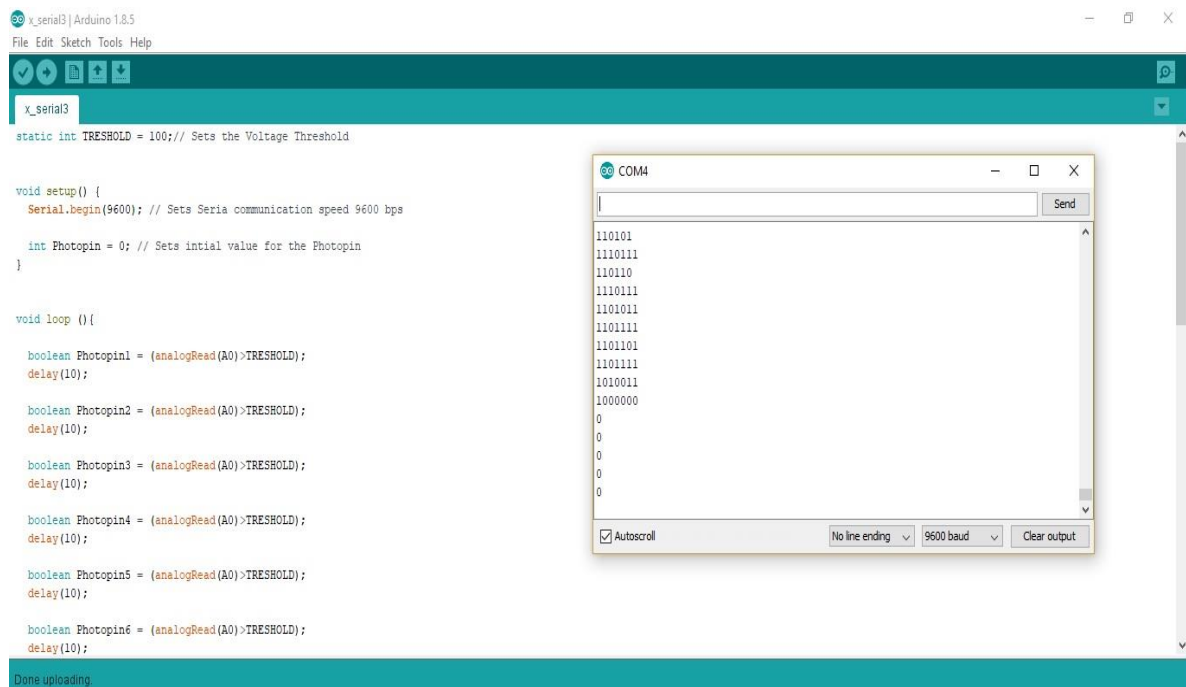
Figure 6.12 0's displayed at the Rx-PC serial monitor after shielding the transmitter

6.3.1. Data rates and BER Estimation

In this section, the amount of data loss will be evaluated to measure the quality of the VLC system. According to the transmitter, code C.1., the amount of 7bits is send in 10m second time, which means that the data rate is approximately 1.42 Kbps. This data rate could be varied by changed by reducing the delay time in the code. The percentage of data loss was measured at varied data rates at a fixed distance of 150 cm from the transmitter. Figure 6.13 shows the percentage of data loss Vs data rate. By increasing the transmission speed more data is lost due to the microcontroller process delay [51], which causes loss of synchronization between the Tx and Rx and therefore more data loss.
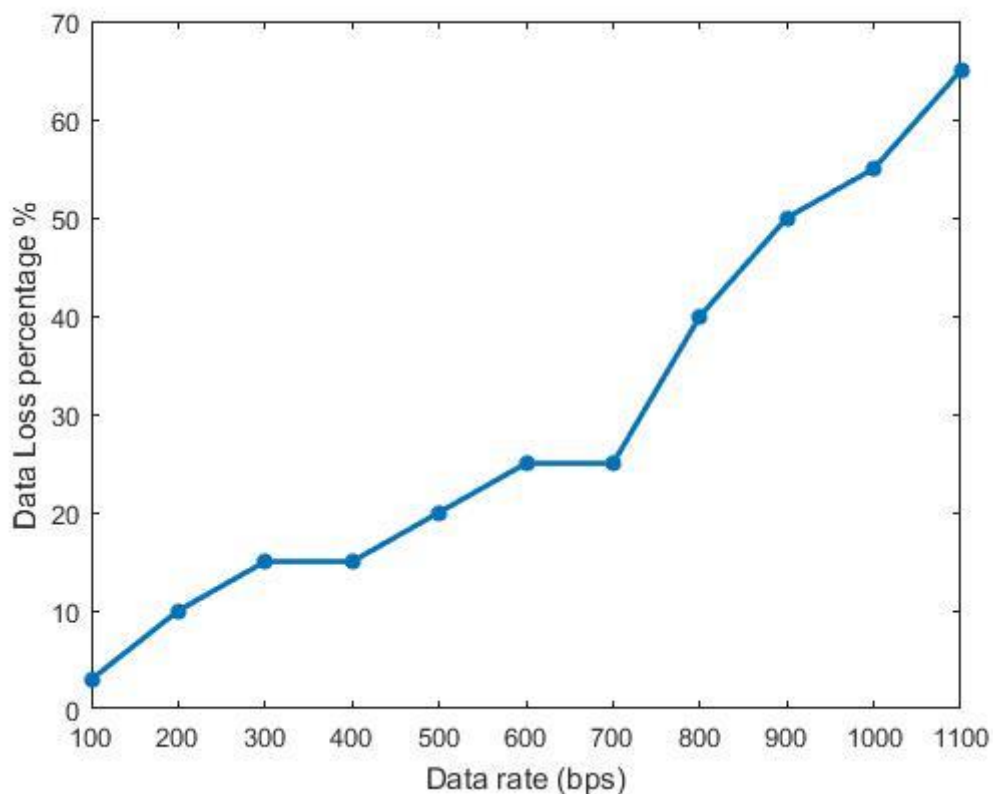
Figure 6.13 Data loss percentage Vs data rate

6.4. Summary

In this chapter the ability of the proposed VLC system to transmit serial data was tested. Modulation and demodulation was carried using Arduino microcontroller boards. The transmitter and receiver designs were explained. First the system was simulated using Autodesk Circuits simulation tool. A suitable algorithm for encoding digital data was created. Laboratory experiments showed that the VLC system is able to transmit serial data with low data loss at a speed of 100 bps however, at higher data rates more data is lost. The low transmission speed and high data loss is due to the speed limitation of the Arduino board.

7. Conclusions and Future work

7.1.   Conclusions

The aim of this study is to Design and implement a tuned Analog Front-End for extending VLC transmission range. This work was focused on Analog electronic design and laboratory based. The first part of this thesis analyzed important factors limiting VLC transmission range and proposed solutions for improving the receiver sensitivity and reducing indoor ambient lights interference. The application of the MFB band pass filter to extend the VLC transmission range was proposed and simulated. An OOK-based tuned AFE employing a fourth order MFB active band pass filter was designed and implemented. Experimental results showed that the implemented receiver was not only able to extend the transmission range but can also reduce the effect of fluorescent lights interference. The system performance was measured in terms of SNR over transmission distance. A 20kbps data rate over a distance of 2m with a BER of 4.89×10^{-10} was successfully achieved by using our proposed inexpensive components. By using the same proposed MFB filter and an additional comparator stage another long-range VLC system based on PWM was designed and implemented. The system was able to achieve a data rate of up to 10Kbps over a transmission range of 4.7m with a low power white LED for transmission, with the presence of ambient light noise background, however the real BER could not be estimated due to inability of demodulation. Another prototype was designed and implemented to test the ability of the proposed VLC system to transmit serial data from PC to PC. The prototype used Arduino Uno Microcontrollers and was able to send data characters from PC to PC over a transmission range of 1.5m with low data loss for data rates below 1Kbps. The limitation of the Arduino system speed returns to low processing speed of the ATMEGA 328P board used which causes synchronization between the transmitter and receiver.

7.2.   Future work and improvements

Future works should be directed towards applying suitable modulation schemes which could comply with the proposed filtering stage characteristics in order to achieve data rates according to the IEEE 802.15.7 standard. The ability of using high power LEDs to achieve longer-range communication and testing the system performance under the outdoor

scenarios should be investigated. In order to obtain accurate evaluation of the system performance, Field-programmable gate array (FPGA) should be incorporated in the system, through which accurate data rates and BER measurements could be achieved. For the system to be capable to transmit serial data with a reasonable speed, microcontroller boards with higher processor speed should be used. The code used for both data transmission and reception should include precise modulation procedure with the ability to adjust the data rate and transmission frequency according to the filtering stage. Finally, the code used to transmit characters should follow the American Standard Code for Information Interchange (ASCII).

References:

[1] Z. Ghassemlooy, L. Alves, S. Zvanovec and M. Khalighi, *Visible light communications*.

[2] A. Pradana, N. Ahmadi and T. Adionos, "Design and implementation of visible light communication system using pulse width modulation", in *ICEEI*, Denpasar, 2015, pp. 25 - 30.

[3] M. Basha and R. Binns, "DC biased input stage with differential photocurrent sensing for VLC front-ends", in *ICCSS*, London, 2017, pp. 167 - 170.

[4] S. Sharma, DESIGN & IMPLEMENTATION OF VISIBLE LIGHT COMMUNICATION SYSTEM. Tallinn, 2017, pp. 41-44.

[5] IEEE Standard for Local and Metropolitan Area Networks—Part 15.7: Short-Range Wireless Optical Communication Using Visible Light, IEEE Standard 802.15.7, 2011.

[6] H. Chen, C. Wu, H. Li, X. Chen, Z. Gao, S. Cui, and Q. Wang. (2016). Advances and prospects in visible light communications. *J. Semiconductors*. [Online]. *37(1)*. Available:

[7] M. Figueiredo, L. N. Alves and C. Ribeiro, "Lighting the Wireless World: The Promise and Challenges of Visible Light Communication," in *IEEE Consumer Electronics Magazine*, vol. 6, no. 4, pp. 28-37, Oct. 2017.

[8] D. Karunatilaka, F. Zafar, V. Kalavally and R. Parthiban, "LED Based Indoor Visible Light Communications: State of the Art," in *IEEE Communications Surveys & Tutorials*, vol. 17, no. 3, pp. 1649-1678, thirdquarter 2015.

[9] R. A. Shaikh, A. Basit, "Using point-to-point 1550nm laser for outdoor mobility", Information and Communication Technologies, 2009. ICICT, pp. 255-258.

[10] Jing Li and M. Uysal, "Achievable information rate for outdoor free space optical communication with intensity modulation and direct detection," *Global Telecommunications Conference, 2003. GLOBECOM '03. IEEE*, 2003, pp. 2654-2658 vol.5.

[11] A. Akbulut, H. G. Ilk and F. Ari, "Design, availability and reliability analysis on an experimental outdoor FSO/RF communication system," *Proceedings of 2005 7th International Conference Transparent Optical Networks, 2005.*, 2005, pp. 403-406 Vol. 1.

[12] Y. F. Huang *et al.*, "17.6-Gbps universal filtered multi-carrier encoding of GaN blue LD for visible light communication," *2017 Conference on Lasers and Electro-Optics (CLEO)*, San Jose, CA, 2017, pp. 1-2.

[13] A. Jovicic, J. Li and T. Richardson, "Visible light communication: opportunities, challenges and the path to market," in *IEEE Communications Magazine*, vol. 51, no. 12, pp. 26-32, December 2013.

[14] "Infrared data association," Walnut Creek, CA, USA, 2012. [Online]. Available: http://www.irda.org

[15] K. Pujapanda, "LiFi integrated to power-lines for smart illumination cum communication," in *Proc. Int. Conf. CSNT*, Gwalior, India, 2013,pp. 875–878

[16] M. Kavehrad, "Sustainable energy-efficient wireless applications using light," *IEEE Commun. Mag.*, vol. 48, no. 12, pp. 66–73, Dec. 2010.

[17]] S. Zhao, J. Xu, and O. Trescases, "A dimmable LED driver for Visible Light Communication (VLC) based on llc resonant DC-DC converter operating in burst mode," in *Proc. 28th Annu. IEEE APEC Expo.*, Long Beach, CA, USA, 2013, pp. 2144–2150.

[18] M. Oh, "A flicker mitigation modulation scheme for visible light communications," in *Proc. 15th ICACT*, Pyeong Chang, Korea, 2013, pp. 933–936.

[19] X. Li, B. Hussain, L. Wang, J. Jiang and C. P. Yue, "Design of a 2.2-mW 24-Mb/s CMOS VLC Receiver SoC With Ambient Light Rejection and Post-Equalization for Li-Fi Applications," in *Journal of Lightwave Technology*, vol. 36, no. 12, pp. 2366-2375, June15, 15 2018.

[20]] H. Chun et al., "LED Based Wavelength Division Multiplexed 10 Gb/s Visible Light Communications," in *Journal of Light wave Technology*, vol. 34, no. 13, pp. 3047-3052, July1, 1 2016.a

[21] C. W. Hsu, C. W. Chow, I. C. Lu, Y. L. Liu, C. H. Yeh and Y. Liu, "High Speed Imaging 3×3 MIMO Phosphor White-Light LED Based Visible Light Communication System," in *IEEE Photonics Journal*, vol. 8, no. 6, pp. 1-6, Dec. 2016.

[22] T. Adiono, A. Pradana, R. V. W. Putra and S. Fuada, "Analog filters design in VLC analog front-end receiver for reducing indoor ambient light noise," *2016 IEEE Asia Pacific Conference on Circuits and Systems (APCCAS)*, Jeju, 2016, pp. 581-584.

[23] M. Basha, M. Sibley and P. Mather, "Design and implementation of a tuned Analog Front-end for extending VLC transmission range", in *IEEE International Conference on Computing, Electronics & Communications Engineering 2018 (iCCECE '18)*, 2018, pp. 173-176.

[24] Breed, G. (2005). *Analyzing Signals Using the Eye Diagram*. [ebook] Available at: http://highfreqelec.summittechmedia.com/Nov05/HFE1105_Tutorial.pdf [Accessed 25 May 2018].

[25] A M Street, P N Stavrinou, D C Obrien and D J Edwards, Indoor optical wireless systems—A review, *Optical and Quantum Electronics*, 29, 349–378, 1997

[26] S Hranilovic, On the design of bandwidth efficient signalling for indoor wireless optical channels, *International Journal of Communication Systems*, 18, 205–228, 2005

[27] Ghassemlooy, W. Popoola and S. Rajbhandari, *Optical wireless communications*, 1st ed. Boca Raton, FL: CRC Press, 2013.

[28] Z. Wu, C. You and C. Yang, "Research on long-range real-time visible light communications over phosphorescent LEDs", in *CCDC*, Chongqing, 2017, pp. 5838 - 5842.

[29] F. Chang, W. Hu and D. Lee, "Design and implementation of anti-low-frequency noise in visible light communications", in *ICASI*, Sapporo, 2017, pp. 1536 - 1538.

[30] S. Rajagopal, R. Roberts and S. Lim, "IEEE 802.15.7 visible light communication: modulation schemes and dimming support", *IEEE Communications Magazine*, vol. 50, no. 3, pp. 72-82, 2012.

[31] G. Ntogari, T. Kamalakis, J. Walewski and T. Sphicopoulos, "Combining Illumination Dimming Based on Pulse-Width Modulation With Visible-Light Communications Based on Discrete Multitone," in *IEEE/OSA Journal of Optical Communications and Networking*, vol. 3, no. 1, pp. 56-65, January 2011.

[32] T. Yamazato *et al.*, "Image-sensor-based visible light communication for automotive applications," in *IEEE Communications Magazine*, vol. 52, no. 7, pp. 88-97, July 2014.

[33] Boyina, S.R.; Deepa, K.; Hari, P.L.; Vivek, S.; Nanda, K.S.; Rajendhiran, A.; Saravana, J. Indoor navigation system for visually impaired person using GPS. *Int. J. Adv. Eng. Technol.* **2012**, 3, 40–43.

[34] P. Huynh, J. Lee and M. Yoo, "An indoor environment VLC-based localization algorithm for handset devices," *2015 Seventh International Conference on Ubiquitous and Future Networks*, Sapporo, 2015, pp. 139-140.

[35] L. Li, P. Hu, C. Peng, G. Shen, and F. Zhao, "Epsilon: A visible light based positioning system," in *Proc. 11th USENIX Symp*. NSDI, Seattle, WA, USA, 2014, pp. 331–343.

[36] A. Jovicic, J. Li, and T. Richardson, "Visible light communication: opportunities, challenges and the path to market," *IEEE Commun. Mag.*, vol. 51, no. 12, pp. 26–32, Dec. 2013.

[37] I. Sahnoun, I. S. Ansari, M. Abdallah and K. Qaraqe, "Performance analysis of adaptive modulation in underwater visible light communications," *2017 25th International Conference on Software, Telecommunications and Computer Networks (SoftCOM)*, Split, 2017, pp. 1-6.

[38] "Nichia NSDL570GS-K1, 5mm-LED, 23lm, 2700K", *Lumitronix.com*, 2018. [Online]. Available: https://www.lumitronix.com/en_gb/nichia-nsdl570gs-k1-5mm-led-23lm-2700k-15037.html. [Accessed: 01-Aug- 2018]

[39] F. Schill, U. R. Zimmer, and J. Trumpf, "Visible spectrum optical communication and distance sensing for underwater applications," in *Proc. ACRA*, Canberra, ACT, Australia, 2004, pp. 1–8.

[40] Anthony C. Boucouvalas, Kostas P. Peppas, K. Yiannopoulos, Z. Ghassemlooy, "Underwater optical wireless communications with optical amplification and spatial diversity," *IEEE Photonics technology letters*, vol. 28, no.22, Nov. 2016.

[41] N. Anous, M. Abdallah, M. Uysal and K. Qaraqe, "Performance Evaluation of LOS and NLOS Vertical Inhomogeneous Links in Underwater Visible Light Communications," in *IEEE Access*, vol. 6, pp. 22408-22420, 2018.

[42] C. Wang, H. Y. Yu and Y. J. Zhu, "A Long Distance Underwater Visible Light Communication System With Single Photon Avalanche Diode," in *IEEE Photonics Journal*, vol. 8, no. 5, pp. 1-11, Oct. 2016.

[43] S. Gray, *Analysis and Design of Analog Integrated Circuits WIE, 4th Edition*, 1st ed. John Wiley & Sons, 2003.

[44] M. Carthy and B. Milpitas, *Precision, High Speed, JFET Input Operational Amplifiers*. 1994.

[45] A. Hussein and A. Abd, "Design and simulation of 4 th order active bandpass filter using multiple feed back and Sallenkey topologie", *Journal of Babylon University/Engineering Sciences*, vol. 22, no. 2, pp. 2155-2157, 2014.

[46] N. Aldibbiat and Z. Ghassemlooy, "Artificial-light-interference effects on indoor optical wireless links employing DH-PIM", *Journal of Optical Networking*, vol. 5, no. 2, p. 103, 2006.

[47] E. Alaybeyoğlu and F. Ugranlı, "A new approach for electronic design automation of analog building blocks," *2018 26th Signal Processing and Communications Applications Conference (SIU)*, Izmir, Turkey, 2018, pp. 1-4.

[48] Lee,   Chung   Ghiu.   (2011).   Visible   Light   Communication.   10.5772/16034. https://www.researchgate.net/publication/221905781_Visible_Light_Communication.

[49] Wu, X. & Zhai, G. Temporal psychovisual modulation: A new paradigm of information display. *IEEE Signal Process. Mag.* **30**, 136–141 (2013).

[50] "Alexander Graham Bell's Photophone: An Invention Ahead of Its Time", *ThoughtCo*, 2018. [Online]. Available: https://www.thoughtco.com/alexander-graham-bells-photophone-1992318. [Accessed: 09- Jun-2018].

[51] W. Stallings and T. Case, *Business Data Communications*. Harlow, United Kingdom: Pearson Education Limited, 2012.

Appendices

Appendix 1 Arduino codes:

C.1. Transmitter Code

```
void setup() {
  Serial.begin(9600); // Sets Serial communication speed 9600 bps
  pinMode(4,OUTPUT); // Sets pin 4 as digital output
}
void loop() {
   Serial.println("START COMMUNICATION!!!");// Begin sending Data
  WriteChar('a');
  WriteChar('b');
  WriteChar('c');
  WriteChar('d');
}
void WriteChar(char str){
  switch (str - '0'){
    case 49:
      //code for a is 011 0001
      LightFlash(false, true, true, false, false, false, true);
      break;
    case 50:
      //code for b is 011 0010
      LightFlash(false, true, true, false, false, true, false);
      break;
    case 51:
      //code for c is 011 0011
      LightFlash(false, true, true, false, false, true, true);
      break;
    case 52:
      //code for d is 011 0100
      LightFlash(false, true, true, false, true, false, false);
      break;
  }
}
void LightFlash(boolean a, boolean b, boolean c, boolean d, boolean e,
boolean f, boolean g){

  digitalWrite(4,LOW);
  if (a == true){
    digitalWrite(4,HIGH);
  }
 delay(10);
  digitalWrite(4,LOW);
  if (b == true){
    digitalWrite(4,HIGH);
  }
  delay(10);
  digitalWrite(4,LOW);
  if (c == true){
    digitalWrite(4,HIGH);
  }
  delay(10);
  digitalWrite(4,LOW);
  if (d == true){
    digitalWrite(4,HIGH);
  }
  delay(10);
  digitalWrite(4,LOW);
```

```
  if (e == true){
    digitalWrite(4,HIGH);
  }
  delay(10);
  digitalWrite(4,LOW);
  if (f == true){
    digitalWrite(4,HIGH);
  }
  delay(10);
  digitalWrite(4,LOW);
  if (g == true){
    digitalWrite(4,HIGH);
  }
  delay(10);
}
```

C.2. Receiver Code

```
static int TRESHOLD = 300;// Sets the Voltage Threshold
void setup() {
  Serial.begin(9600); // Sets Seria communication speed 9600 bps
  int Photopin = 0; // Sets intial value for the Photopin
}
void loop (){
  boolean Photopin1 = (analogRead(A0)>TRESHOLD);
  delay(10);
  boolean Photopin2 = (analogRead(A0)>TRESHOLD);
  delay(10);
  boolean Photopin3 = (analogRead(A0)>TRESHOLD);
  delay(10);
  boolean Photopin4 = (analogRead(A0)>TRESHOLD);
  delay(10);
  boolean Photopin5 = (analogRead(A0)>TRESHOLD);
  delay(10);
  boolean Photopin6 = (analogRead(A0)>TRESHOLD);
  delay(10);
  boolean Photopin7 = (analogRead(A0)>TRESHOLD);
  delay(10);
  long result = 0;
  result = 1000000*Photopin1 + 100000*Photopin2 + 10000*Photopin3
  + 1000*Photopin4 + 100*Photopin5 + 10*Photopin6 + 1*Photopin7;
  PrintChar(result);
  Serial.println(result);
}
void PrintChar(long binary){
  switch (binary){
    case 110001:
      //code for a is 011 0001
      Serial.println("a");
      break;
    case 110010:
      //code for b is 011 0010
      Serial.println("b");
      break;
    case 110011:
      //code for c is 011 0011
      Serial.println("c");
      break;
    case 110100:
      //code for d is 011 0100
```

74

```
        Serial.println("d");
        break;

    case 11000:
        Serial.println("Debug 1: character not recognised");// Setting Error
message
        break;
    case 1011001:
        Serial.println("Debug 2: character not recognised");
        break;
    case 100001:
        Serial.println("Debug 3: character not recognised");
        break;
    case 1011000:
        Serial.println("Debug 4: character not recognised");
        break;
    }
}
```
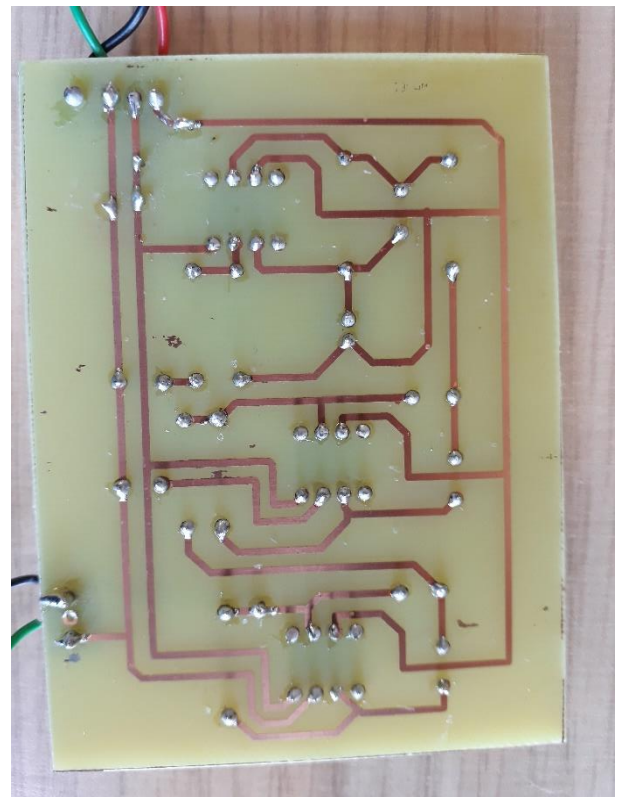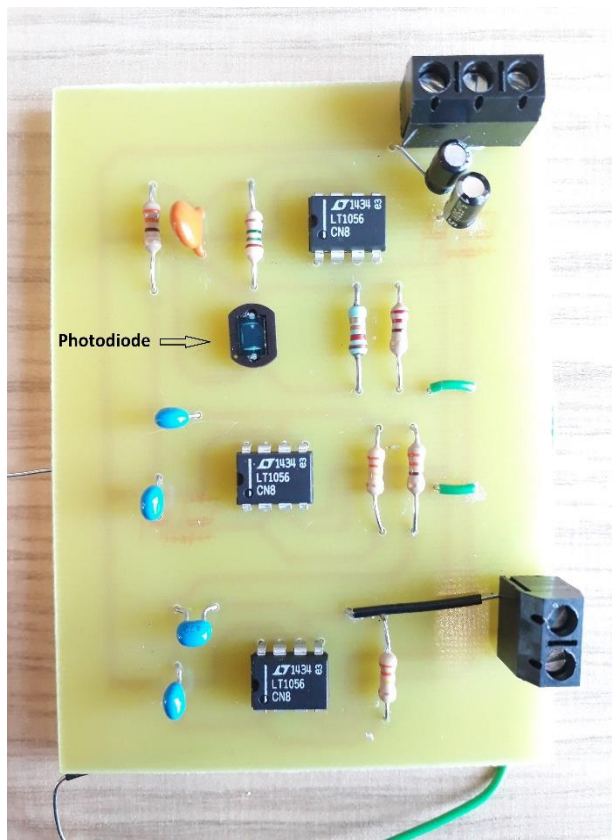
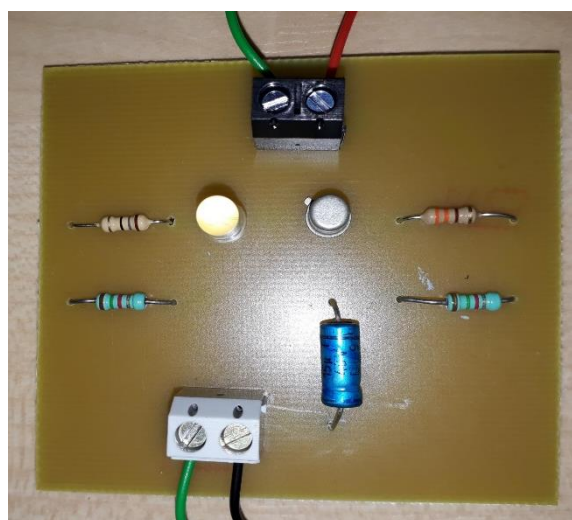## Appendix 2 Prototypes for VLC system using Manchester coding
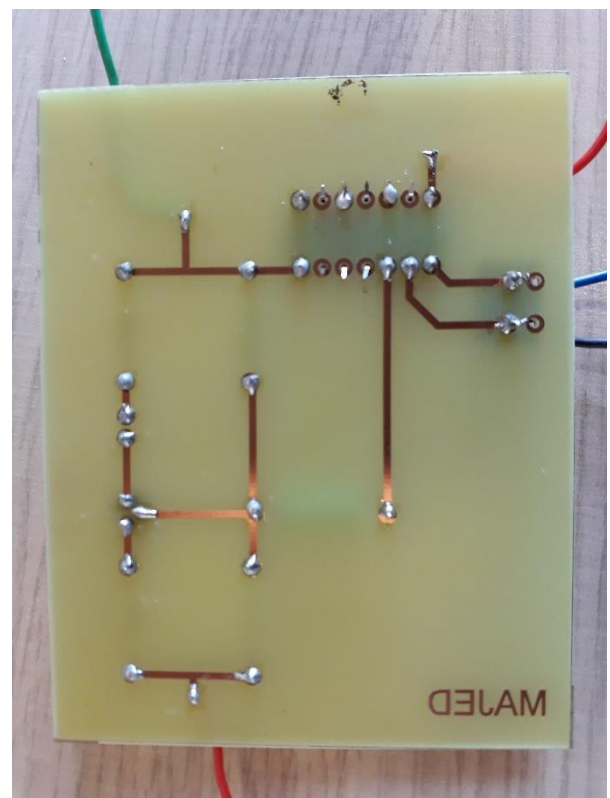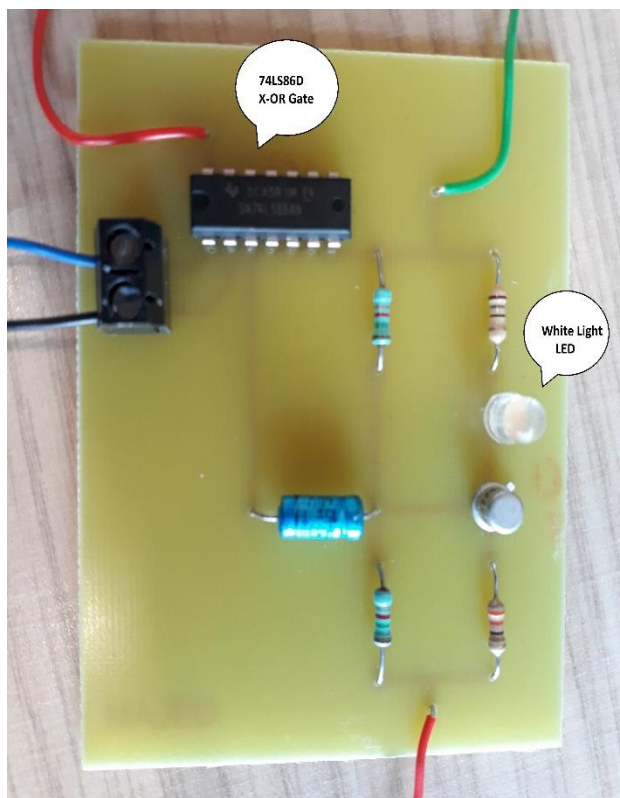
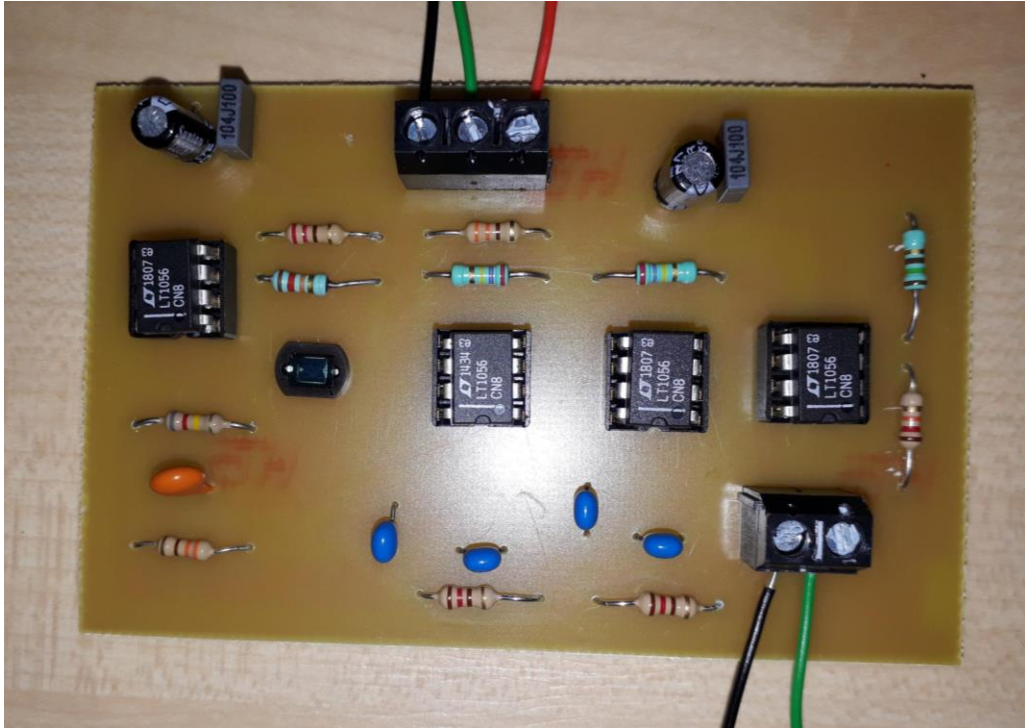Final PCB prototype of the Manchester coding transmitter

Receiver circuit implemented on PCB

Appendix 3 Prototypes for VLC system using PWM

LED driver circuit final prototype

Final PCB of propose PWM receiver circuit